© 2016. Published by The Company of Biologists Ltd | Development (2016) 143, 595-608 doi:10.1242/dev.127175

RESEARCH ARTICLE

# Differential regulation of mouse and human nephron progenitors by the Six family of transcriptional regulators

**Lori L. O'Brien[1], Qiuyu Guo[1,2], YoungJin Lee[1,*], Tracy Tran[1], Jean-Denis Benazet[1,‡], Peter H. Whitney[1], Anton Valouev[2,§] and Andrew P. McMahon[1,§]**

## ABSTRACT

Nephron endowment is determined by the self-renewal and induction of a nephron progenitor pool established at the onset of kidney development. In the mouse, the related transcriptional regulators Six1 and Six2 play non-overlapping roles in nephron progenitors. Transient Six1 activity prefigures, and is essential for, active nephrogenesis. By contrast, Six2 maintains later progenitor self-renewal from the onset of nephrogenesis. We compared the regulatory actions of Six2 in mouse and human nephron progenitors by chromatin immunoprecipitation followed by DNA sequencing (ChIP-seq). Surprisingly, *SIX1* was identified as a SIX2 target unique to the human nephron progenitors. Furthermore, RNA-seq and immunostaining revealed overlapping SIX1 and SIX2 activity in 16 week human fetal nephron progenitors. Comparative bioinformatic analysis of human SIX1 and SIX2 ChIP-seq showed each factor targeted a similar set of cis-regulatory modules binding an identical target recognition motif. In contrast to the mouse where Six2 binds its own enhancers but does not interact with DNA around *Six1*, both human SIX1 and SIX2 bind homologous *SIX2* enhancers and putative enhancers positioned around *SIX1*. Transgenic analysis of a putative human *SIX1* enhancer in the mouse revealed a transient, mouse-like, pre-nephrogenic, *Six1* regulatory pattern. Together, these data demonstrate a divergence in SIX-factor regulation between mouse and human nephron progenitors. In the human, an auto/cross-regulatory loop drives continued SIX1 and SIX2 expression during active nephrogenesis. By contrast, the mouse establishes only an auto-regulatory Six2 loop. These data suggest differential SIX-factor regulation might have contributed to species differences in nephron progenitor programs such as the duration of nephrogenesis and the final nephron count.

**KEY WORDS: Nephrogenesis, Nephron, Regulatory network, Six1/2, Transcription**

## INTRODUCTION

Nephrons are the major functional unit of the kidney, filtering the blood to eliminate waste products, maintaining water, salt and pH balance, and regulating blood volume and pressure. A typical human kidney is composed of approximately one million nephrons, although this number ranges considerably (Bertram et al., 2011). The final human nephron number is established prior to birth; nephrogenesis is reported to cease around 36 weeks of gestation (Hinchliffe et al., 1991). Altered renal function and reduced nephron numbers are associated with premature birth and low birth weight, respectively (Mañalich et al., 2000; Rodríguez-Soriano et al., 2005; Hughson et al., 2003). Several studies have shown a link between low nephron number and an increased risk of hypertension late in life (Brenner et al., 1988; Keller et al., 2003; Hughson et al., 2006). An understanding of the determinants of nephron number might facilitate prevention of kidney and kidney-related disease.

In the mouse, all nephrons are derived from a pool of self-renewing metanephric mesenchyme progenitors established around embryonic day (E)10-E10.5 (Kobayashi et al., 2008). This population surrounds the invading epithelial ureteric bud tips of the nascent collecting duct at E11.0 and commences nephrogenesis (Boyle et al., 2008; Kobayashi et al., 2008). At each round of ureteric branching, nephrons are induced by a Wnt9b signal emanating from the ureteric epithelium (Carroll et al., 2005). Wnt9b and other factors also promote the expansion of the progenitor pool (Self et al., 2006; Kobayashi et al., 2008; Karner et al., 2011; Barak et al., 2012; Xu et al., 2014), which undergoes a large increase over the course of nephrogenesis (Short et al., 2014). The nephron progenitor pool persists until postnatal day (P)2-P3; its depletion marks the cessation of nephrogenesis with the generation of around 13,000 nephrons over a 12 day period of active kidney development (Hartman et al., 2007; Rumballe et al., 2011; Cullen-McEwen et al., 2003). Several transcriptional regulators are crucial for establishing or maintaining this population, including Sall1, Wt1, Osr1, Eya1, Pax2, Hox11 paralogs, and two closely related Six-family members, Six1 and Six2 (Kreidberg et al., 1993; Torres et al., 1995; Xu et al., 1999, 2003, 2014; Nishinakamura et al., 2001; Wellik et al., 2002; Li et al., 2003; James et al., 2006; Self et al., 2006; Xu and Xu, 2015).

The founding member of the Six family, *sine oculus* (*so*), was first discovered in *Drosophila melanogaster*, where analysis of mutants established *so* as a major regulator of visual system development (Milani, 1941; Fischbach and Heisenberg, 1981; Fischbach and Technau, 1984; Cheyette et al., 1994; Serikaku and O'Tousa, 1994). Subsequent studies identified two additional family members, *optix* (also known as *D-Six3*) and *D-Six4*, with roles in eye development and mesoderm derivatives, respectively (Seo et al., 1999; Seimiya and Gehring, 2000; Kirby et al., 2001; Kenyon et al., 2005; Clark et al., 2006; Weasner et al., 2007). Vertebrate homologs have been characterized for all three founding members and reveal an additional duplication of each Six gene, giving rise to six mammalian members: Six1-Six6. On the basis of sequence analysis and gene structure, *Six1* and *Six2* diverged from *so*, *Six3* and *Six6* from *optix*, and *Six4* and *Six5* from *D-Six4* (Seo et al., 1999). Six factors bind DNA through a conserved homeodomain whereas the shared Six domain facilitates

[1]Department of Stem Cell Biology and Regenerative Medicine, Broad-CIRM Center, Keck School of Medicine, University of Southern California, Los Angeles, CA 90089, USA. [2]Division of Bioinformatics, Department of Preventative Medicine, Keck School of Medicine, University of Southern California, Los Angeles, CA 90089, USA. *Present address: iDream Research Center, Mizmedi Women's Hospital, Seoul, Republic of Korea. ‡Present address: Department of Developmental and Cell Biology, Weill Cornell Medical College, New York, NY 10065, USA.

§Authors for correspondence (valouev@usc.edu; amcmahon@med.usc.edu)

**Received 3 June 2015; Accepted 23 December 2015**

Development (2016) 143, 595-608 doi:10.1242/dev.127175

interactions with co-regulators such as eya/Eya1 (Pignoni et al., 1997; Seo et al., 1999). Despite the divergence of *Six1* and *Six2* from *so*, neither gene is expressed or functions in the developing mouse eye. Instead *Six1* and *Six2* are expressed in a number of other developing tissues including the otic placode, branchial arches, muscle and kidney (Oliver et al., 1995).

In the developing mouse kidney, transient *Six1* activity in the early kidney rudiment at E10.5 is essential for ureteric bud outgrowth and metanephric mesenchyme survival (Xu et al., 2003; Li et al., 2003; Xu and Xu, 2015) whereas sustained *Six2* activity in the nephron progenitors is essential for their self-renewal, acting, at least in part, to block progenitor commitment to nephrogenesis (Self et al., 2006; Kobayashi et al., 2008; Park et al., 2012). Consequently, a loss-of-function for either gene results in kidney agenesis. The levels of *Six2* are reduced in *Six1* mutants, suggesting *Six1* acts upstream of *Six2* (Xu et al., 2003; Li et al., 2003). Clearly, although not essential for activation of *Six2*, Six1 might play a role in establishing normal *Six2* levels prior to the termination of *Six1* expression around E11.5 (Xu et al., 2003). By that time, Six2 is thought to regulate its own activity through auto-feedback loops mediated by proximal and distal enhancer elements (Brodbeck et al., 2004; Gong et al., 2007; Park et al., 2012). Collectively, these studies demonstrate quite distinct temporal expression patterns and regulatory dynamics for *Six1* and *Six2* in mouse kidney development.

Many of the genes integral for mouse kidney development are associated with renal anomalies in the human population, suggesting close genetic parallels between the two species. Mutations have been identified in a number of genes encoding transcription factors, signaling proteins, and receptors that act within the nephron progenitor niche or the adjacent ureteric epithelium, including EYA1, PAX2, SALL1, RET, BMP4, FGF20, ITGA8, and SIX1 and SIX2 (Müller et al., 1997; Davidson, 2009; Cain et al., 2010; Barak et al., 2012; Humbert et al., 2014).

SIX1 mutations are associated with branchio-oto-renal (BOR) syndrome, whereas SIX2 mutations are linked to isolated cases of renal hypodysplasia (Ruf et al., 2004; Weber et al., 2008), highlighting their crucial roles in human kidney development. Furthermore, SIX1 and SIX2 mutations have also recently been associated with Wilms' tumor, a pediatric kidney cancer (Wegert et al., 2015; Walz et al., 2015). The tumors are characterized by blastemal, epithelial and stromal elements much like the developing kidney. The blastema displays nephron progenitor-like characteristics, expressing factors such as CITED1, SIX1 and SIX2 (Li et al., 2002; Lovvorn et al., 2007; Murphy et al., 2012; Sehic et al., 2012, 2014). Mutations in the DNA binding homeodomain of SIX1 and SIX2 are associated with chemotherapy-resistant blastemas, suggesting that these mutations might contribute to an aggressive etiology of such tumors (Wegert et al., 2015).

Although genetic studies support a common set of regulatory factors underlying mouse and human kidney development, there is clearly a marked difference between their nephron progenitor programs. Whereas the mouse kidney generates around 13,000 nephrons over approximately 2 weeks of active nephrogenesis, the human kidney forms around a million nephrons over a 30 week period of nephrogenesis (Cullen-McEwen, et al., 2003; Bertram et al., 2011). These striking differences between the duration and output of the nephron progenitor pool between mouse and man are likely to reflect different regulatory properties intrinsic to the progenitor pool or within the niche where progenitors reside.

In this study, we explored the intrinsic regulatory programs at play within human nephron progenitors and provide evidence for distinct regulatory programs of Six/SIX between mouse and human kidneys. The data provide a potential mechanistic link to the lengthened period of progenitor self-renewal and nephrogenesis underlying human kidney development.

## RESULTS

Given the crucial role for Six2 in mouse nephron progenitor self-renewal (Self et al., 2006), our previous analysis of Six2-directed regulatory circuitry in nephron progenitors (Park et al., 2012) and the contribution of SIX2 mutations to human renal anomalies (Weber et al., 2008), we examined SIX2 regulatory function in the human fetal kidney. Six2 is highly expressed from E10.5 within the mouse nephron progenitor population, and downregulated upon commitment of progenitors to nephron formation (Oliver et al., 1995; Self et al., 2006; Kobayashi et al., 2008; Mugford et al., 2009; Park et al., 2012) (Fig. 1A). Human kidney development initiates at 5 weeks with the invasion of the ureteric bud and terminates around 36 weeks. Consequently, the 16 week human kidney is approximately one-third of the way through the active period of nephrogenesis, analogous to the E15.5-E16.5 mouse kidney, a developmental stage extensively characterized for Six2 regulation in earlier studies (Park et al., 2012; Kanda et al., 2014). Additionally, the kidney appears to be undergoing active branching until at least 20 weeks of gestation (L.L.O. and A.P.M., unpublished observations).

As in the mouse kidney, human SIX2 displayed a nuclear localization within condensed mesenchyme cells surrounding the ureteric epithelial tips in the outer kidney cortex (Fig. 1A). CITED1, a definitive nephron progenitor marker in the mouse (Boyle et al., 2007; Park et al., 2012), colocalized with SIX2 in this group of cells (Fig. S1A). The overlap of SIX2 and CITED1 was observed in all nephron progenitors, but unlike the mouse, where only Six2 extends into early stages of nephrogenesis, we observed human CITED1 beneath the ureteric branch tips in what are likely to be early-forming nephron structures (Mugford et al., 2009; Park et al., 2012; Fig. S1A). SIX2 activity extended into nascent nephron precursors underneath the ureteric buds. SIX2 expression was downregulated in the differentiating structures and localized proximally in the renal vesicle, which were both similar attributes to mouse Six2 expression (Fig. 1A, bottom panel). Thus, the overall distribution of mouse and human Six2/SIX2 are quite similar, consistent with SIX2 highlighting the human nephron progenitor compartment. Unlike mouse kidneys, human kidneys have an underlying lobular organization. Where the lobes ingress and meet, $SIX2^+$ progenitor niches closely abut each other but appear to maintain their local tip niche integrity with $SIX2^+$ cells closely opposed to tips of the underlying branching ureteric tree (Fig. 1A, zoomed inset).

Next, we performed ChIP-seq on mouse and human kidney tissues to compare regulatory patterns between Six2/SIX2 and identify common and unique transcriptional targets. Human SIX2 binding was analyzed from two independent replicates of 17 week fetal kidney tissues. The QuEST ChIP-seq peak caller (Valouev et al., 2008) identified 54,068 and 1916 peaks, with a highly significant overlap of 1592 shared peaks between the two SIX2 datasets ($P$-value=$10^{-43}$; Fig. S1B). The differing number of peaks was due to lower levels of SIX2 ChIP enrichment in the second replicate (Fig. S1C). Examination of SIX2 binding near *MEOX1* and *WT1* highlighted the similar binding profiles for SIX2 replicates (Fig. 1B). Within the mouse embryonic kidney *Meox1* is localized and restricted to nephron progenitors (Mugford et al., 2009). *Wt1* is expressed more broadly including the progenitors, (Mugford et al., 2009) and is essential for progenitor maintenance (Kreidberg et al.,

Development (2016) 143, 595-608 doi:10.1242/dev.127175

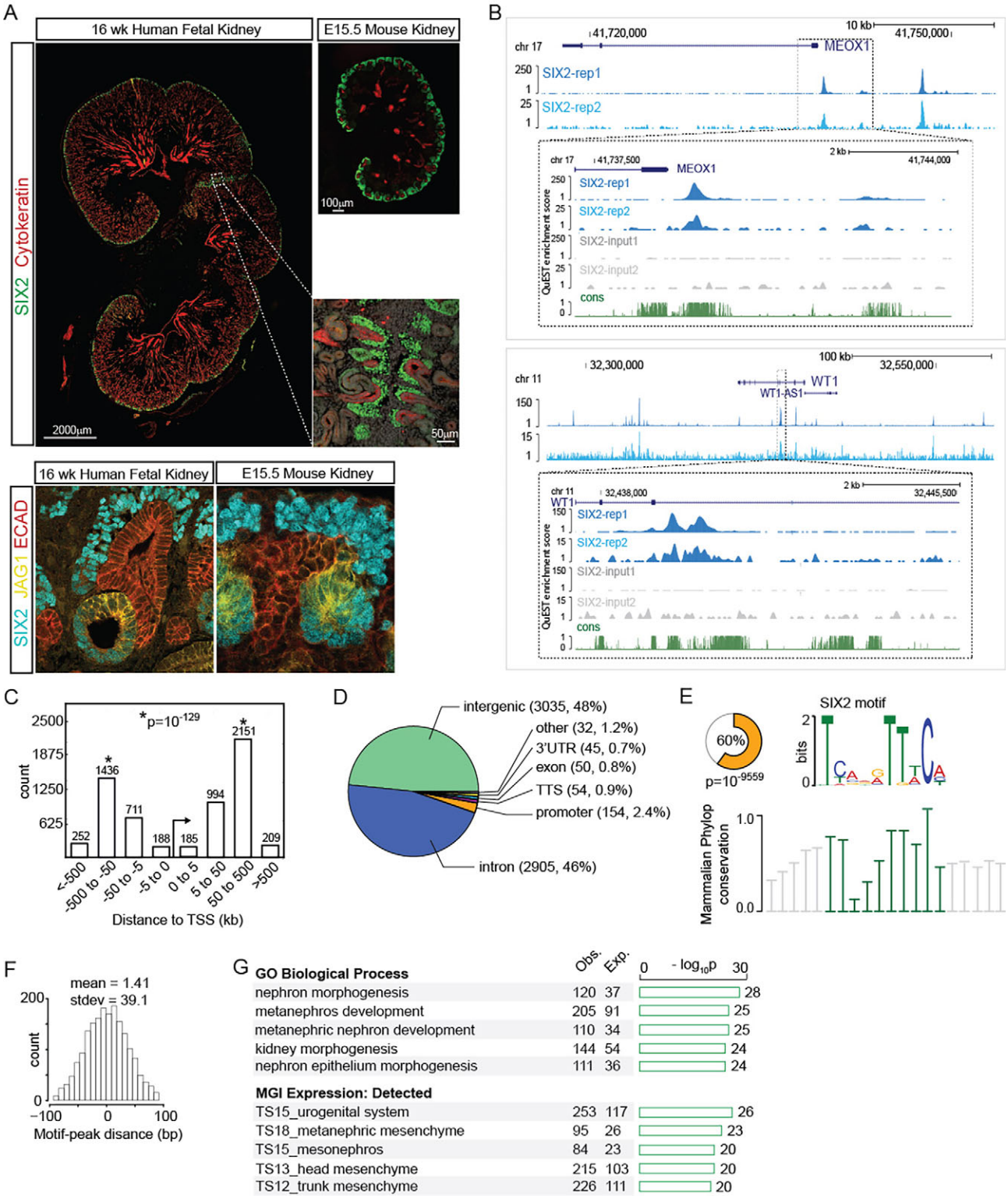


**Fig. 1. Human SIX2 ChIP-seq reveals a kidney-specific regulatory network.** (A) SIX2 and cytokeratin (top), and SIX2, JAG1 and ECAD (bottom) immunostaining of human and mouse fetal kidneys. (B) Genomic view of *MEOX1* and *WT1* loci showing SIX2 peaks. 'cons', Phastcon vertebrates conservation score. (C) Distribution of SIX2 peaks relative to TSSs. **P*-value represents the significance of peaks falling 50-500 kb in either direction from the TSS. (D) Genomic annotation of SIX2 peaks. (E) Weblogo of the most enriched motif (top) and its conservation (bottom). (F) Distribution of SIX2 motif-peak distances. (G) Functional annotation of SIX2 peaks. Obs., observed; Exp., expected.

1993). SIX2 ChIP-seq peaks tended to localize within conserved blocks of DNA consistent with SIX2 binding to the conserved cis-regulatory elements (Fig. 1B). Multiple sites of SIX2 binding are found within *WT1* introns and 100's of kilobases (kb) 5′ and 3′ of the *WT1* transcription unit, suggesting that *WT1* is a major target of SIX2 regulation (Fig. 1B, bottom panel). Given that the reads for the

Development (2016) 143, 595-608 doi:10.1242/dev.127175

two replicates were more strongly correlated when enrichment was compared within rep1 binding regions ($R^2$=0.46 versus 0.19, Fig. S1C), indicating that SIX2-rep1 is a considerably stronger dataset, we restricted further analyses to SIX2-rep1.

Approximately 60% of SIX2 peaks mapped within 50-500 kb of transcriptional start sites (TSSs) (47% randomly expected, *P*-value=$10^{-129}$); very few (<5%) were observed within 5 kb of the promoter (Fig. 1C). Additionally, SIX2 peaks predominantly occurred within intergenic (48%) and intronic (46%) regions, which is a typical pattern of bona fide enhancers (Fig. 1D). We performed a motif search within ±100 bps of the center of the top 1000 Six2 peaks using the *de novo* motif finder MEME (Bailey et al., 2009). The top motif, TCANGTTTCA, closely matches a previously verified Six2 binding motif from FACS sorted nephron progenitors (Park et al., 2012) that mapped to 60% of all SIX2 peaks (Fig. 1E). Motifs were enriched at the peak center as expected for a direct association of SIX2 with DNA (Fig. 1F). Furthermore, calculating the average conservation PhyloP scores (Siepel et al., 2006) across motif bases within SIX2 peaks demonstrated that the high-frequency motif bases tended to also have higher conservation (Fig. 1E). These data highlight the functional significance in the conservation of nucleotides that are likely to mediate DNA-protein contacts (Kumar, 2009).

To further interrogate the biological functions of human SIX2, we performed GREAT GO analysis (McLean et al., 2010) on the ChIP-seq peaks. SIX2 peaks were highly enriched near genes associated with metanephric kidney specific processes such as 'nephron morphogenesis' and 'metanephric development', and predicted a target cell type with an appropriate 'metanephric mesenchyme' and 'urogenital system' gene expression signature (Fig. 1G). In summary, analysis of human SIX2 ChIP-seq data uncovers a robust set of SIX2-bound enhancers within human nephron progenitors supporting a role for SIX2 regulation of nephron progenitor programs in the progenitor niche.

To assess the potential functional similarities and differences between human SIX2 and mouse Six2, we compared human ChIP-seq data with an E16.5 mouse whole kidney Six2 ChIP-seq dataset. The mouse data recovered an identical Six2 binding motif to that of the human SIX2 ChIP-seq data. Similar to human SIX2, a large fraction (43%) of mouse Six2 peaks contained a Six2 motif enriched at peak centers (Fig. 2A,B). Because the mouse and human datasets were roughly comparable in their strength, we used a stricter peak-calling threshold to identify the strongest set of peaks: 12,145 for the mouse kidney and 6276 for the human kidney. In order to compare binding patterns of SIX2/Six2 between the two species, we 'humanized' mouse Six2 peaks by converting mouse peak coordinates to their human counterparts with the UCSC genome browser liftOver tool (Rhead et al., 2010).

Of the 9004 converted mouse Six2 peaks, only 727 sites (~8%) overlapped with human SIX2 peaks with a gap threshold of 100 bp (Fig. 2C). The small degree of peak overlap cannot be attributed to differences in the antibodies used for the human and mouse ChIP-seq comparison, because the two antibodies produce correlated binding data in mouse (Fig. S2A). Reproducible peaks were enriched for kidney target genes and the Six2 motif (Fig. S2B,D) and differential peaks tended to localize close to the TSS of highly active metabolic genes, without kidney specificity and were not enriched for the Six2 motif (Fig S2B,C,D). The finding of low binding site overlap between mouse and human is in line with previous reports comparing transcription factor binding in the same cell or tissue between species (Odom et al., 2007; Kunarso et al., 2010; Schmidt et al., 2010). For example, only 12-14% of the binding sites for CEBPa and HNF4a in the mouse and human liver are conserved; the differences have been attributed to the loss of motifs as a result of sequence changes (Schmidt et al., 2010). SIX2 human/mouse shared sites show the greatest enrichment for the SIX2 motif, 65% compared with 59% (human unique) and 21% (mouse unique), and the strongest conservation of the recovered binding motif (Fig. 2C). Furthermore, shared peaks had better enrichment of GO terms associated with kidney function such as 'urogenital system development' and 'metanephros development'. These terms were absent from unique peak sets (Table S2). These observations argue that shared mouse-human sites have stronger functional roles compared with peaks observed in only one species. Interestingly, despite a relatively small overlap of Six2 binding sites between mouse and human, over 50% of putative Six2 target genes are shared between the two species (Fig. 2D). These results support the idea that Six2 binding is more conserved at the level of target genes, compared with conserved binding at individual enhancers. Therefore, new Six2 sites have probably evolved near the same target genes, contributing to regulatory and species diversity.

As suggested by the GO analysis, the overlap of mouse and human binding sites was enriched for potential target genes associated with kidney functions (Table S2). This includes genes that have integral roles in mouse kidney development and associate with human renal abnormalities, such as *SALL1*, *EYA1* and *SIX2* (Abdelhak et al., 1997; Kohlhase et al., 1998; Xu et al., 1999; Nishinakamura et al., 2001; Self et al., 2006; Weber et al., 2008). Our previous study showed that *Eya1* is a direct target of Six2 (Park et al., 2012) acting through an enhancer that is also conserved and bound by human SIX2 (asterisk in Fig. S3). Additionally, several other potential enhancer modules around *EYA1*/*Eya1* are conserved between the two species (Fig. S3). These data highlight the conservation of cis-regulatory modules around genes with important roles in kidney development.

To discover potential novel Six2/SIX2 targets in mouse and human nephron progenitors, we utilized a combination of target regulatory potential and expression data. The regulatory potential measure is based on the number of peaks near each gene and the strength of the peaks (Tang et al., 2011). We first set out to identify genes with marked disparity in SIX2 regulatory potential between mouse and human nephron progenitors (Fig. 2E, left panel, Tables S2 and S3). As expected, *SIX2* is a strong putative target of its own regulation in both mouse and human (Park et al., 2012; Fig. 2E, Tables S2 and S3). Surprisingly, one of the most highly regulated targets of human SIX2 was *SIX1* (Fig. 2E, Tables S2 and S3). In the mouse, *Six1* expression is lost shortly after *Six2* is turned on (Xu et al., 2003) and therefore is an unlikely target. In agreement with this, *Six1* had the lowest possible regulatory potential in mouse, as expected from its temporally restricted expression profile (Xu et al., 2003; Fig. 2E, Tables S2 and S3). These data also indicated that Six2 is not likely to directly repress *Six1*. Thus, *SIX1* appears as a human-specific target by analysis of regulatory potential.

To further narrow down the list of genes identified as species-specific targets by regulatory potential, we examined their expression in human and mouse nephron progenitors to identify targets that also have species-specific expression. We performed RNA-seq on FACS isolated ITGA8$^+$ cells from 17 week human fetal kidney cortex and E15.5 Cited1$^+$ nephron progenitors. ITGA8 is expressed in the nephron progenitors and induced structures of the kidney (Müller et al., 1997; Fig. S4A). We utilized a limited enzymatic digestion of the human fetal kidney to isolate cells from the outer cortical layers in a procedure that recovers ITGA8$^+$

Development (2016) 143, 595-608 doi:10.1242/dev.127175

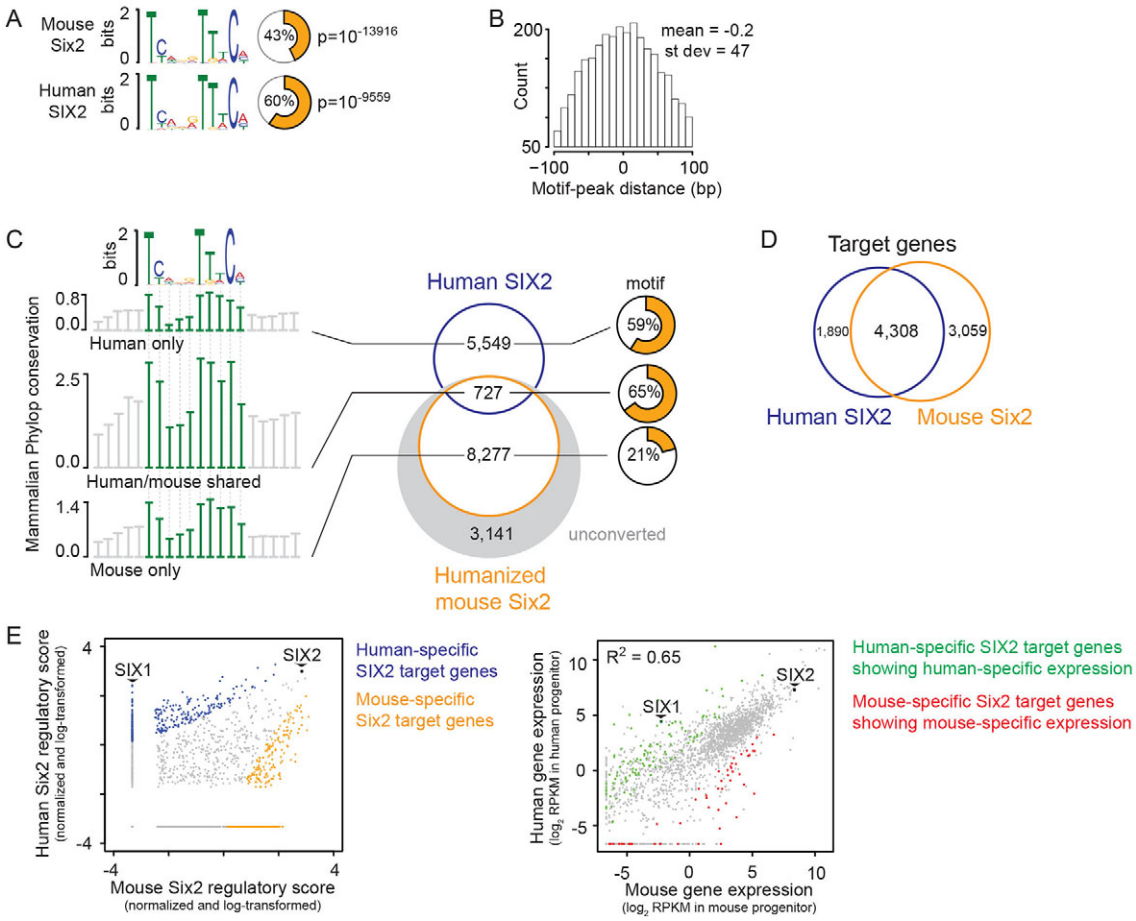


**Fig. 2. Mouse and human SIX2 share many common targets but *SIX1* represents a unique human target.** (A) Comparison of the most enriched motif for Six2/SIX2 peaks. (B) Distribution of Six2 motif-peak distances. (C) Overlap between human SIX2 binding sites and converted mouse Six2 binding sites with mammalian Phylop conservation (left) and peak percentages with motifs (right). (D) Overlap of human and mouse SIX2 target genes. (E) (Left) Human/mouse target genes plotted by their SIX2/Six2 regulatory scores. (Right) Nephron progenitor-specific expression of all conserved genes from human and mouse. Genes identified as species-specific targets with species-specific expression are marked.

nephron progenitors but excludes the majority of differentiating structures (Fig. S4A). Using RNA-seq data from nephron progenitors, we compared expression of genes between human and mouse and identified genes that were >5-fold enriched in either species and were also a species-specific target (Fig. 2E, right panel, highlighted genes). *SIX1* is expressed in the human ITGA8$^{+}$ progenitors, but not in mouse nephron progenitors, identifying *SIX1* as a human specific target on the basis of both cis-interactions around the *SIX1* gene and active *SIX1* expression (right panel Fig. 2E; Table S3).

We examined epigenetic chromatin signatures around *SIX1*/*Six1* and *SIX2*/*Six2* genomic regions in both species to identify regulatory differences that might contribute to species differences in *SIX1*/*Six1* expression. ChIP-seq was performed on 17 week fetal kidneys and E16.5 mouse kidneys to assess chromatin marks associated with active genes and enhancers (H3K27ac) and transcriptionally silenced chromatin (H3K27me3). In the human fetal kidney, the *SIX2* locus displayed a similar profile to that of the mouse: bound by SIX2 at conserved elements and marked by H3K27ac in both the gene body and at SIX2-bound regions (Fig. 3B). Similarly, the human *SIX1* locus was bound by SIX2 at multiple conserved elements and displayed prominent H3K27ac throughout the gene body and the SIX2-bound regions (Fig. 3A). By contrast, the mouse *Six1* locus did not show significant binding by Six2 or H3K27ac enrichment but was marked by a strong H3K27me3 signal (Fig. 3A), which is consistent with epigenetic silencing of the region. Together, these findings indicate a transcriptionally active human *SIX1* state and suggest that *SIX1* expression might be regulated, at least in part, through direct SIX2-mediated transcriptional activation.

Previous immunodetection studies reported SIX1 localization in the condensed mesenchyme of the 17-20 week human fetal kidney (Li et al., 2002; Sehic et al., 2012). However, SIX1 and SIX2 are highly conserved in their DNA-binding and SIX domains (Fig. S4C); consequently, the potential for crossreactivity of antibodies between SIX proteins clouds this interpretation. To definitively examine SIX1 localization in the developing human kidney, we utilized a C-terminal-specific antibody that uniquely recognizes SIX1 (Fig. S4B). At 16 weeks of fetal development, nuclear SIX1 was readily identified within nephron progenitors throughout the many nephron progenitor niches established following the onset of ureteric branching 11 weeks earlier (Fig. 4A). Furthermore, SIX1 and SIX2 proteins showed a highly similar distribution in human nephron progenitors (Fig. 4A). By contrast, mouse Six1 and Six2 overlapped in the metanephric mesenchyme at E10.5, but Six1 was absent from nephron progenitors by E11.5 (Fig. 4B). However, Xu et al. (2003) observed *Six1* activity at E11.5 through a *lacZ* knock-in allele. Because *Six1* activity was measured indirectly, this finding is

Development (2016) 143, 595-608 doi:10.1242/dev.127175

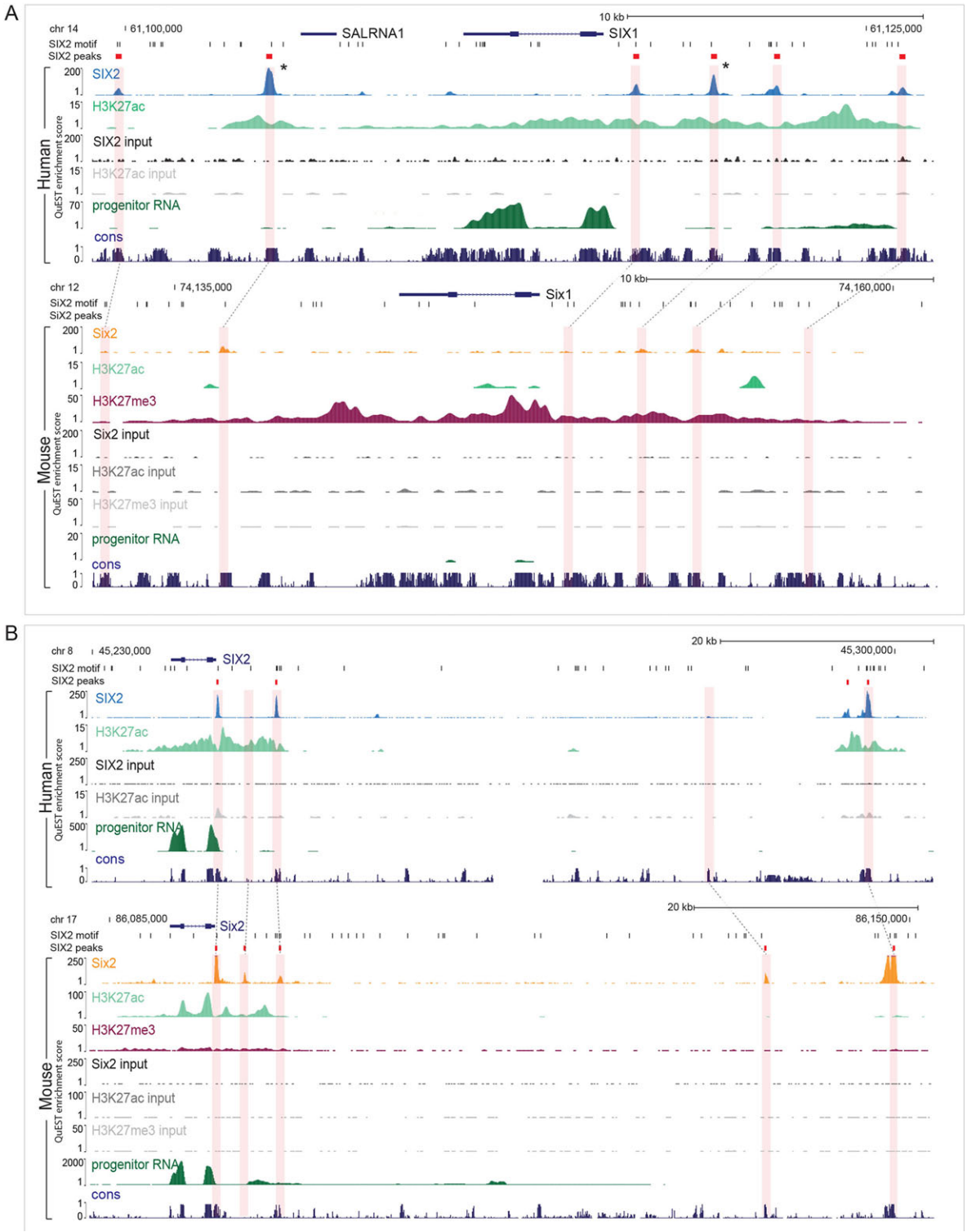


**Fig. 3. *SIX1* is active and regulated by SIX2 in human but not mouse nephron progenitors.** Genomic view of (A) human *SIX1* (top) and mouse *Six1* (bottom) loci and (B) human *SIX2* (top) and mouse *Six2* (bottom) loci. Cons, Phastcon vertebrate conservation score. Asterisks indicate samples used for transgenic assays.

likely to reflect perdurance of β-galactosidase activity following silencing of *Six1*.

Because *Six1* and *Six2* are transiently co-expressed in the E10.5 metanephric mesenchyme, we asked whether *Six1* expression was dependent on Six2 at this stage. We examined Six1 expression in $Six2^{GCE/+}$ and $Six2^{GCE/GCE}$ mouse kidneys that harbor a mutant allele generated by knock-in of a GFP cassette into the *Six2* locus (Kobayashi et al., 2008). In both heterozygous and *Six2*-null mutants, we observed co-labeling of GFP and Six1 in the metanephric mesenchyme, with similar levels of Six1 staining between the two genotypes (Fig. 4C). Therefore, *Six1* activity is not dependent on Six2 in the metanephric anlagen. Furthermore,

Development (2016) 143, 595-608 doi:10.1242/dev.127175

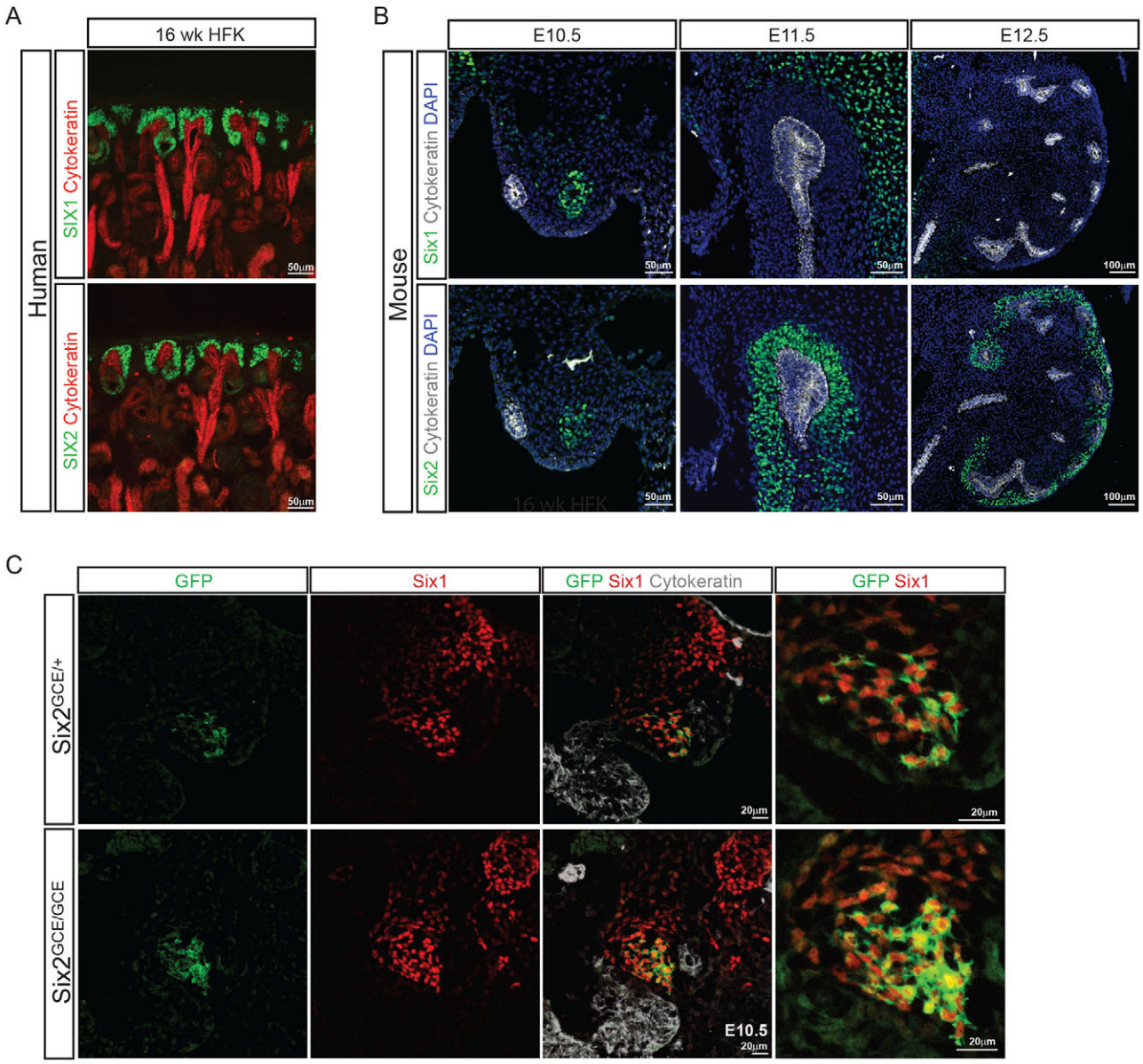


**Fig. 4. Six1 expression is transient and independent of Six2 in the mouse whereas it persists in human nephron progenitors.** (A) SIX1, SIX2 and cytokeratin immunostaining of sectioned human fetal kidney (HFK) (B) Six1, Six2 and cytokeratin immunostaining of adjacent sections from E10.5, E11.5 and E12.5 mouse kidneys. (C) GFP, Six1, and cytokeration immunostaining of E10.5 *Six2*$^{GCE/+}$ and *Six2*$^{GCE/GCE}$ kidneys. Images on far right show zoomed 2views.

although all GFP$^{+}$ cells were SIX1$^{+}$, there were many more cells that had Six1 expression but lacked GFP signal. This suggests that *Six1* activation precedes and is independent of Six2, consistent with a requirement for *Six1* in the E10.5 kidney and the more severe *Six1* mutant phenotype (Xu et al., 2003; Li et al., 2003; Self et al., 2006; Xu and Xu, 2015).

The SIX2-bound regions near the human *SIX1* locus might serve as enhancers maintaining *SIX1* expression in the human fetal kidney. To examine the regulatory activity of these regions, we selected the two strongest SIX2-bound conserved modules within the *SIX1* locus (Fig. 3A, asterisks) and tested a single copy of each for enhancer activity in a G0 mouse transgenic assay scoring for activation of a *lacZ::nGFP* fusion cassette. The strongest enhancer (Enh1) lies in an intergenic region ~11.5 kb downstream of the *SIX1* promoter, and displays high conservation across vertebrates (Fig. 3A). The second strongest enhancer (Enh2) lies ~4 kb upstream of the *SIX1* promoter within another highly conserved block (Fig. 3A). These two enhancers were previously confirmed to be regulatory elements controlling *Six1* expression in the developing mouse embryo (Sato et al., 2012). Enh1 and Enh2 both showed activity in the otic vesicle and cranial ganglia, reported sites of *Six1* expression (Sato et al., 2012) (Fig. 5A). Enh1 showed additional activity in the olfactory placode, eye and apical ectodermal ridge of the developing limb bud. However, only Enh2 showed highly reproducible metanephric mesenchyme-specific expression at E10.5 (0/3 for Enh1, 6/9 for Enh2; Fig. 5A), similar to their mouse equivalents (Sato et al., 2012). When Enh1 was analyzed at E15.5, 1/17 transgenic positive kidney pairs displayed a nephron progenitor-specific expression pattern, whereas 3/17 displayed additional distinct β-gal$^{+}$ patterns (Fig. 5B,C; Fig. S5). For Enh2,

Development (2016) 143, 595-608 doi:10.1242/dev.127175

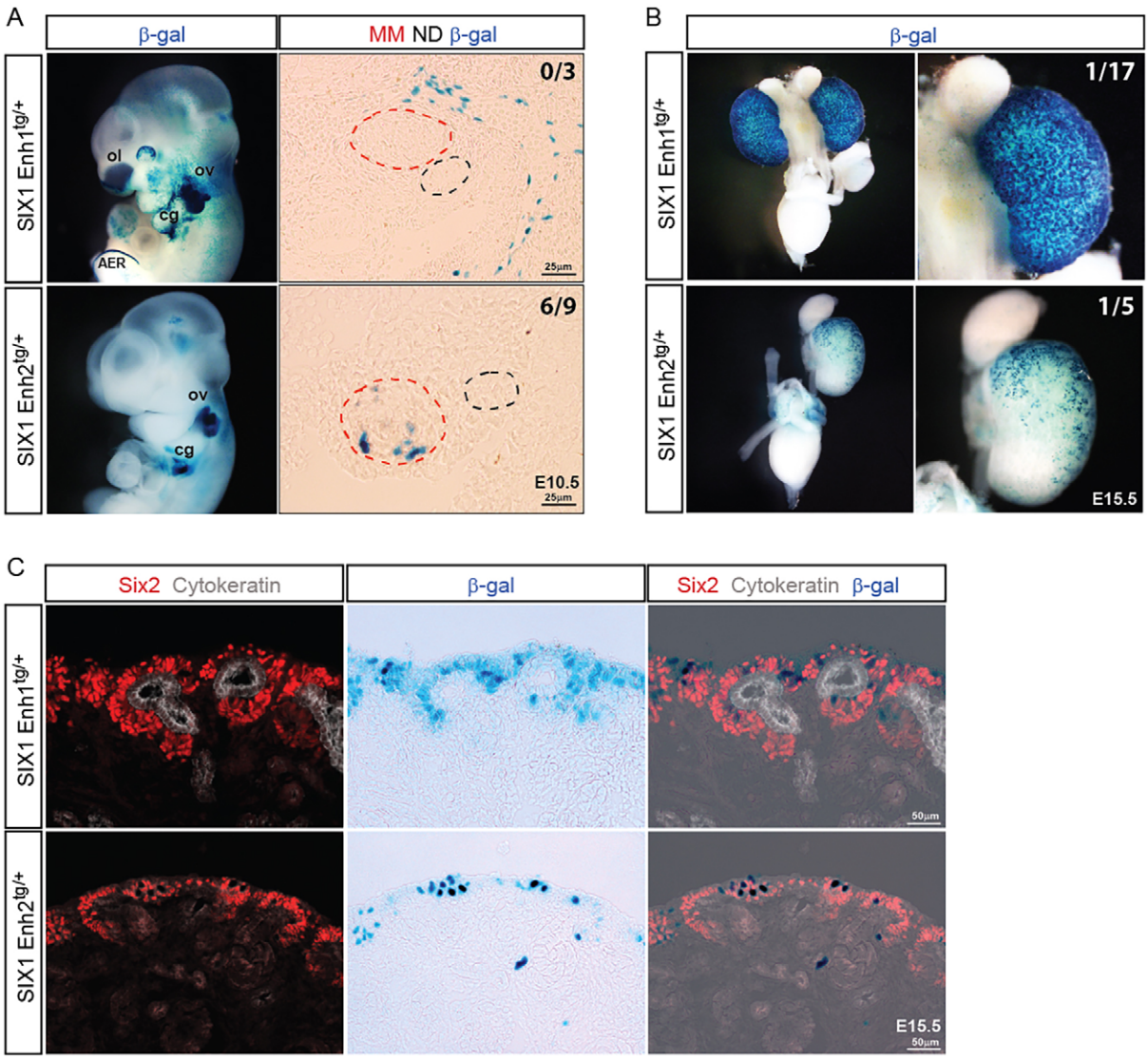


**Fig. 5. Transgenic mouse analysis of human *SIX1* enhancers shows similar regulation to mouse *Six1* in the developing mouse kidney.** (A) β-galactosidase (β-gal) activity of the two *SIX1* enhancers at E10.5. Number of *lacZ*$^{+}$ transgenics showing MM expression at E10.5 is indicated. cg, cranial ganglia; ov, otic vesicle; ol, olfactory placode; AER, apical ectodermal ridge; MM, metanephric mesenchyme; ND, nephric duct. (B) β-gal activity of the two *Six1* enhancers at E15.5. Number of transgenics showing nephron progenitor expression is indicated. (C) Six2 and cytokeratin staining of kidney sections from B.

1/5 transgenic kidney pairs showed a mosaic expression that mapped specifically to nephron progenitors (Fig. 5B,C). In summary, only Enh2 showed robust activity in the mouse metanephric mesenchyme at E10.5, whereas both enhancers showed sporadic nephron progenitor activity at E15.5 when mouse *Six1* was inactive. Collectively, these data highlight early active enhancer elements switched on prior to active nephrogenesis that are mostly, but not always, shut down in later nephron progenitors (see Discussion).

To directly address the functional role of SIX1 in the human fetal kidney, we performed SIX1 ChIP-seq on 16 and 17 week kidney replicates. The two datasets showed moderate overlap and were correlated (Fig. S6A,B). To remove potential false-positive SIX1 peaks, we focused on the overlapping set of 1610 sites. *De novo* motif recovery identified a peak-centered motif matching the SIX2 motif, consistent with the highly conserved DNA-binding homeodomain of SIX1 and SIX2 and previous SIX1 ChIP data from C2C12 myoblast cells (Liu et al., 2012; Fig. 6A,B; Figs S4C and S6C). The 1610 overlapping SIX1 peaks had a SIX motif recovery rate of 60%, similar to the SIX2 peaks (Fig. 6A) and higher than each individual SIX1 ChIP-seq replicate (43% and 38%, Fig. S6A), supporting the specificity of the shared SIX1 peaks and indicating that the strongest peaks within each dataset lie within the overlap. Thus, SIX1 and SIX2 recognize the same DNA binding motif and consequently, each factor is likely to target a common set of enhancers and regulate a common set of genes in the nephron progenitor pool.

Consistent with this prediction, an overwhelming majority of SIX1 peaks (~81%) were shared with SIX2 peaks, and their binding strengths were significantly correlated ($R^2$=0.4; Fig. 6C,E). Additionally, nearly all predicted SIX1 target genes (~90%) were shared with SIX2 (Fig. 6D). SIX1-only peaks had lower signals compared with shared peaks (Fig. S6E), indicating that they represent peaks where SIX2 signals fall below the detection threshold rather than being truly unique sites. The C-terminal regions of SIX1/2 protein sequences are divergent and could lead to

Development (2016) 143, 595-608 doi:10.1242/dev.127175

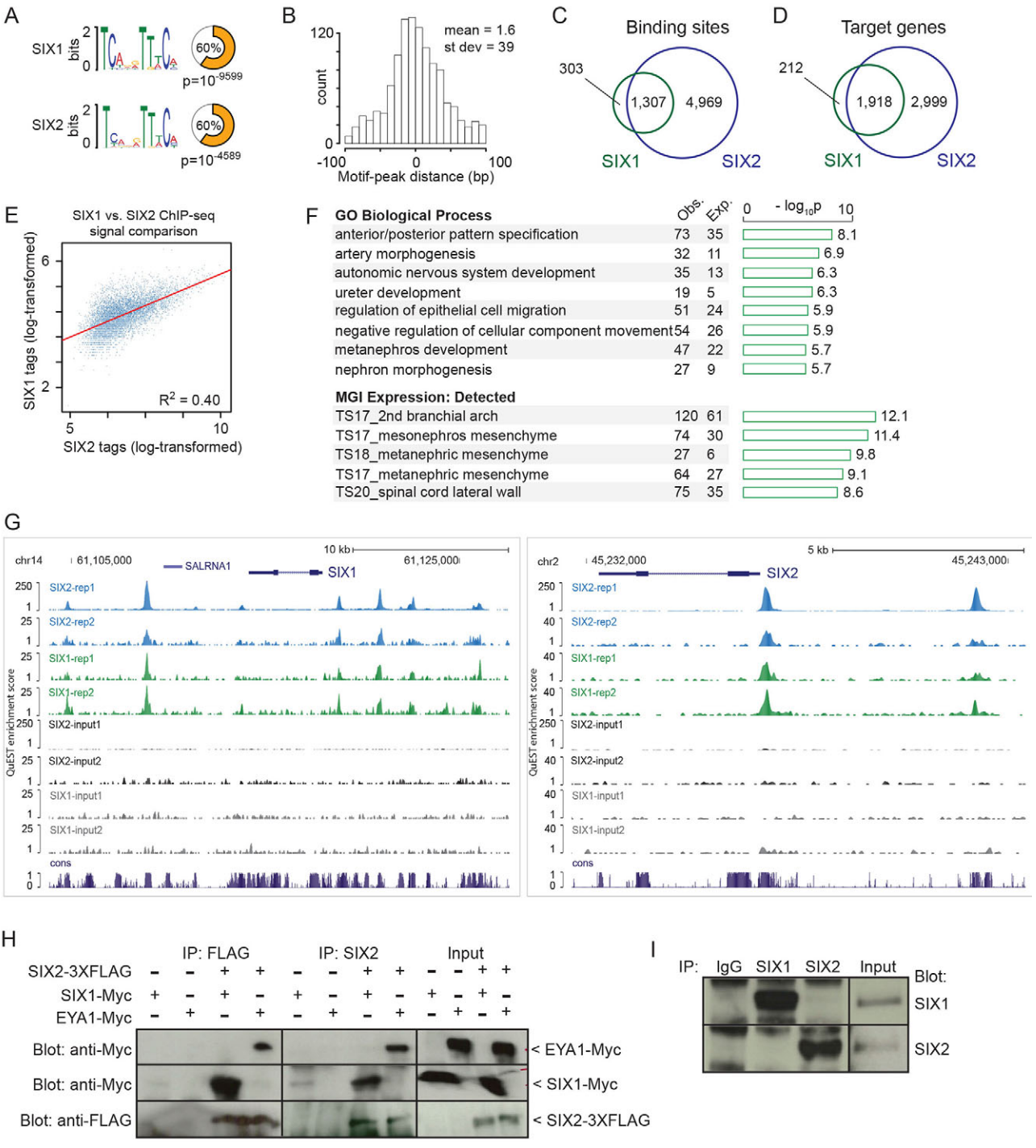


**Fig. 6. SIX1 and SIX2 share common targets and show evidence of auto- and cross-regulatory activity.** (A) Comparison of the most enriched motif for SIX1 and SIX2 peaks. (B) Distribution of SIX1 motif-peak distances. (C) Overlap of SIX1 and SIX2 binding sites. (D) Overlap of SIX1 and SIX2 target genes. (E) Comparison of raw signals from SIX2 and SIX1 ChIP-Seq data sets. Each point represents a single binding peak. (F) Gene ontology analysis of shared SIX1/SIX2 peaks. Obs., observed; Exp., expected. (G) Genomic view of the human *SIX1* (left) and *SIX2* (right) gene loci. (H) Western blot of SIX2-3×FLAG co-immunoprecipitations from HEK293 cells. (I) Western blot of SIX1 and SIX2 co-immunoprecipitations from human fetal kidneys.

differing protein-protein interactions (Fig. S4C), which might influence levels of SIX1 and SIX2 recruitment to their target sites through interactions with differing co-factors. This idea is supported by a relatively low correlation (0.18) between SIX1 and SIX2 signals across the shared peaks (Fig. S6D). Motif recovery on the shared and non-overlapping peaks identified a WT1-like motif and E-box motif in both the overlapping and SIX2 only sites (Fig. S6F), suggesting that WT1 and a bHLH factor are potential binding partners of SIX1 and SIX2. The 303 SIX1-unique sites yielded a SIX motif, but no WT1 or E-box signals. The lack of co-factor motifs amongst Six1-only sites is most likely due to the low number of peaks and low enrichment of these peaks (Fig. S6E,F). Whether SIX1 and SIX2 interact with different co-factors at independent target sites remains an open question.

Development (2016) 143, 595-608 doi:10.1242/dev.127175

GREAT GO analysis of the overlapping SIX1-SIX2 peaks revealed an association with kidney processes such as 'metanephros development' and expression of the targets in kidney associated structures such as 'metanephric mesenchyme' (Fig. 6F). Predicted target genes include *SIX1*, *SIX2*, *SALL1*, *WT1* and *OSR1* (Table S4). Taken together, these data indicate that SIX1 and SIX2 recognize a very similar set of enhancers for the same targets in human nephron progenitors mediated through interactions with a common SIX-type motif. Importantly, these interactions include co-regulatory inputs at their own and each other's enhancers (Fig. 6G).

These findings leave open the possibility that both factors are simultaneously engaged within a common regulatory complex. To address this, we performed co-immunoprecipitations from HEK293 cells transfected with tagged proteins. First, as a positive control, we confirmed that SIX1 and SIX2 complex with EYA1 (Fig. 6H, data not shown), in agreement with previous studies using fly and mouse homologs (Pignoni et al., 1997; Buller et al., 2001). Next, we analyzed whether SIX1 and SIX2 interact with each other. Whereas, SIX1 and SIX2 were co-immunoprecipitated using specific antibodies for distinct epitope tags following overexpression in HEK293 cells (Fig. 6H, SIX1 data not shown), SIX1 and SIX2 were not co-immunoprecipitated by SIX1- and SIX2-specific antibodies in extracts of 17 week human kidney (Fig. 6I). The results indicate that either (1) the antibodies used for immunoprecipitation *in vivo* disrupt the heterodimeric SIX1-SIX2 complex or (2) SIX1 and SIX2 form independent transcriptional complexes *in vivo* that are capable of associating with the same regulatory elements in human nephron progenitors, but ectopically, SIX1 and SIX2 can form complexes when present at high levels in a heterologous cell type. To distinguish between these possibilities, we repeated the co-immunoprecipitation analysis in HEK293 cells using the SIX2-specific antibody from the *in vivo* studies. In HEK293 cells, SIX2 and SIX1 co-immunoprecipitated indicating the SIX2-specific antibody does not disrupt the *in vitro* generated SIX1-SIX2 complex (Fig. 6H). Taken together, these results support the presence of independent SIX1 and SIX2 regulatory complexes *in vivo*, although we cannot rule out the possibility of some minor role for less-stable SIX1-SIX2 complexes that might be highlighted by *in vitro* overexpression conditions.

## DISCUSSION

### Comparison of human and mouse SIX2/Six2 functions

In this study we examined the conservation of human and mouse SIX2/Six2 expression and function. We observed that localization of SIX2 within nephron progenitors is similar in the developing mouse and human fetal kidney. A majority of the SIX2/Six2 transcriptional targets are shared between the two species, demonstrating a common set of SIX2/Six2 target genes despite a relatively low overlap of binding peaks at the homologous enhancers. Additionally, the *in vivo* recovered motif bound by Six2/SIX2 is identical in mouse and human progenitors, in agreement with conserved DNA-binding domains. Given that their Six/SIX domains and C-terminal domains are also highly similar, protein-protein interactions mediated through these regions are also likely to be conserved between the two species.

A recent study has shown that conserved sites bound by transcription factors in mouse and human are correlated with pleiotropic functions (Cheng et al., 2014). These enhancers are active across multiple tissues, subjecting them to strong evolutionary constraints that preserve motifs within enhancer modules. The authors suggest that the conserved, pleiotropic enhancers might be bound by transcription factors within the same family that recognize the same motif (Cheng et al., 2014). In our data, the conservation of the SIX2 motif is highest amongst shared sites of human and mouse binding and enhancers are conserved around target genes such as *EYA1*/*Eya1*. Eya1 is integral for the proper development of several tissues, including the kidney, inner ear, cranial ganglia and branchial arch derivatives (Xu et al., 1999, 2002; Zou et al., 2004). It would be interesting to determine whether our prospective enhancers are also active in these additional tissues. Six1 and Six2 are expressed in many of these same tissues, consistent with a multi-tissue regulatory link (Oliver et al., 1995; Sato et al., 2012).

Whereas the target genes and function of SIX2 appear to be highly conserved, we identified *SIX1* as a novel and unique target of SIX2 in the human fetal kidney. Our analyses uncovered other gene targets predicted through regulatory potential and expression analyses to show species-specific patterns of progenitor activity. Other than SIX1, our data identifies several additional genes that have high expression in the human kidney ITGA8$^{+}$ cells versus mouse nephron progenitors, and have higher regulatory potential in the human versus mouse (Table S3). Similar to *SIX1*, such genes represent unique regulatory targets of SIX2 in human. Examples of such genes include *COL6A2* and *CDH7*, suggesting potential differences in matrix and cell-cell adhesions between human and mouse nephron progenitors. Conversely, *Hs3st6*, a heparin sulfate sulfotransferase and Wt1 target (Motamedi et al., 2014), represents a mouse-specific Six2 target gene with higher expression in mouse Cited1$^{+}$ nephron progenitors (RPKM=35.640) but low expression (RPKM=0.225) in the ITGA8$^{+}$ human nephron progenitor-enriched population. Confirmation of species-specific expression of these genes and their potential differential impact on mouse and human nephron progenitor functions will be a focus for future studies.

### SIX1 function in mouse versus human

*Six1* is required for maintenance of the early metanephric mesenchyme (Xu et al., 2003; Li et al., 2003; Xu and Xu, 2015), but by the time the first round of branching has occurred in the mouse, Six1 is no longer detectable. However, SIX1 activity extends far beyond the initial round of branching, and overlaps with SIX2 in human nephron progenitors. These findings raise the questions of (1) how mouse and human differentially regulate their Six-genes during kidney development, and (2) what is the functional significance of their divergent regulatory programs?

Clearly, a common regulatory theme for mouse Six2 and human SIX1/2 are their auto-regulatory activities. Each factor binds its own gene's progenitor-specific enhancer; in addition, human SIX1 and SIX2 cross-regulate *SIX2* and *SIX1* genes, respectively. However, their initial activation in the early-specified metanephric anlagen is likely to be dependent on other factors. In the mouse, our data demonstrate that *Six1* activation is independent of *Six2* and that *Six1* acts upstream of *Six2*, in line with previous reports showing that *Six1* is required for normal *Six2* expression (Xu et al., 2003; Li et al., 2003). The situation in the equivalent stage of human kidney development (4.5-5 weeks) is presently unknown (Fig. 7).

Examination of transgenic activity of human *SIX1* (this paper) and mouse *Six1* (Sato et al., 2012) enhancer modules suggests that initial activating mechanisms might be regulated through a common enhancer, and this module and potentially others, promotes persistent SIX factor-mediated nephron progenitor expression of human SIX1. In this scenario, enhancer silencing within the mouse *Six1* locus through activities of additional

Development (2016) 143, 595-608 doi:10.1242/dev.127175

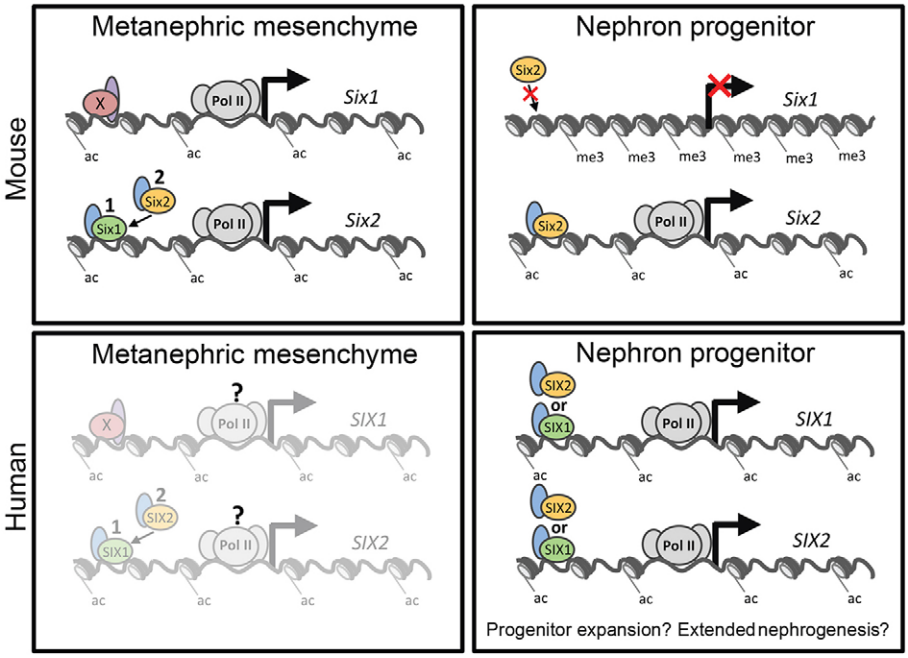


**Fig. 7. Model of differential regulation of Six1/2 and SIX1/2 in the developing mouse and human kidney.** In the metanephric mesenchyme of the mouse (E10.5), *Six1* expression is driven by factor (s) 'X' and is actively transcribed (Pol II). Six1 can then activate *Six2* expression (1), and subsequently Six2 can drive its own expression (2) via an autoregulatory loop. Because both loci are active, they are marked by H3K27ac (ac). However, in the mature nephron progenitors, *Six1* is no longer expressed and displays a repressive histone signature of H3K27me3 (me3). Six2 cannot access the *Six1* enhancers and continues to drive its own expression. In the human metanephric mesenchyme (~5 weeks of gestation), the expression and regulation of *SIX1* and *SIX2* are unknown. In mature nephron progenitors and in contrast to the mouse, *SIX1* is active and expression is driven by SIX2 and itself. Similarly, *SIX2* expression is driven by SIX1 and itself. SIX1 and SIX2 are likely to regulate expression through discrete complexes.

regulators would presumably block engagement of Six1 and Six2, resulting in early down-regulation of *Six1* in the mouse. In the human kidney, such enhancer silencing activities are absent and both *SIX1* and *SIX2* expression persists in nephron progenitors through weeks of highly active nephrogenesis (Fig. 7). Alternatively, human *SIX1* might utilize distinct regulatory elements not shared with the mouse and excluded from Enh2 that maintain *SIX1* expression in human nephron progenitors after the initial activating trigger is lost.

The human *SIX1* enhancers show the most robust and consistent activity at E10.5, with Enh2 displaying metanephric mesenchyme activity at E10.5, overlapping endogenous *Six1* expression (Xu et al., 2003). However, their reporter expression patterns become variable with rare activity by E15.5. Whereas over 50% of transgenic mice show activity from a *Six2* distal enhancer (Park et al., 2012; L.L.O. and A.P.M., unpublished data), only 6-20% show activity from the human enhancers at this time. This suggests that human enhancers are subject to similar regulation to their mouse Six1 regulatory counterparts but might escape that regulation in some transgenic lines where the transgene integration site could influence the expression outcome. Importantly, as SIX1/2 binding motifs are conserved between mouse and human in both enhancers (Fig. 3A), the differing regulatory outcomes for mouse *Six1* and human *SIX1* do not appear to result from the loss of Six-specific binding elements.

In mouse nephron progenitors at E16.5, the *Six1* locus is marked by an H3K27me3 signature indicative of PRC2-mediated transcriptional silencing. When and how this silencing occurs remains to be determined. In the mouse, *Six2* progenitor expression extends until depletion of the nephron progenitors at the end of the nephrogenic period (Hartman et al., 2007; Rumballe et al., 2011). The temporal expression patterns of SIX1 and SIX2 throughout human nephrogenesis are currently unclear. SIX2 expression in human fetal kidney progenitors has been reported at 24 weeks of development but nephrogenesis continues until 36 weeks (Murphy et al., 2012).

The functional significance of distinct *Six1/SIX1* regulation between mouse and human is a matter for speculation at this time. Clearly, Six1 and Six2 are key regulators of nephron progenitors (Xu et al., 2003; Li et al., 2003; Self et al., 2006; Xu and Xu, 2015), and Six2 maintains and expands progenitors by countering progenitor commitment to nephrogenesis (Self et al., 2006; Kobayashi et al., 2008; Park et al., 2012). One attractive model posits a dual action for SIX1 and SIX2 in modifying progenitor programs to extend the period of progenitor expansion. Overexpression of SIX2 in a nephroblastoma cell line increases the number of cells in S-phase (Senanayakea et al., 2013), supporting the idea that elevated levels of SIX proteins enhance cellular proliferation and progenitor expansion. SIX2 is expressed at higher levels than SIX1 in the ITGA8$^{+}$ progenitor-enriched population (157.12 RPKM versus 21.57 RPKM, respectively; Table S3) suggesting that SIX2 remains the predominant SIX factor in nephron progenitors. A relatively small change in SIX levels could have significant ramifications in the balance of progenitor numbers. Furthermore, recent evidence suggests that OSR1/Osr1, which shows comparable expression levels to SIX1 in both human and mouse (RPKMs of 16.21 and 32.01, respectively; Table S3), acts synergistically with Six2 to maintain the nephron progenitors (Xu et al., 2014). Additional experimental studies will be required to explore the significance of human SIX1 in expanding nephron progenitors.

Six2 and its human SIX counterparts also bind enhancers that activate expression of genes encoding key signals promoting progenitor differentiation such as *Fgf8* and *Wnt4*, suggesting a role for Six/SIX factors in the control of progenitor commitment (Park et al., 2012 and data therein). Ultimately, the period of progenitor activity depends on a balance of progenitor renewal and commitment, altering the dynamics of either process will influence the size of the nephron progenitor pool and the duration of nephrogenesis. The extended lifetime of the human nephron progenitor pool is likely to be a key factor in the 100-fold greater number of nephrons formed in the human versus the mouse kidney. Further mechanistic insights might be gained from examining regulation of *Six1/2* and regulatory activity in experimental mammalian models with a nephrogenic period and nephron count closer to the human kidney.

Development (2016) 143, 595-608 doi:10.1242/dev.127175

### SIX1/2 in cell programming and Wilms' tumor

Recent reports have shown that SIX1 and SIX2 are both required to reprogram human proximal tubule cells to nephron progenitors (Hendry et al., 2013), suggesting that SIX1 might have additional non-overlapping functions with SIX2. Alternatively, absolute levels of SIX proteins might be important, and high levels are required for reprogramming and progenitor maintenance. SIX1/2 mutations have recently been associated with Wilms' tumors (Wegert et al., 2015; Walz et al., 2015). These data provide further evidence that the blastemal elements of the tumor reflect the characteristics of the nephron progenitor niche. Interestingly, Wegert et al. (2015) performed SIX1 ChIP-seq on tumor samples with and without the SIX1 mutation. The motif recovered from the wild-type tumor data, GAAACCTGATCC, closely matches the TGAAACCTGA recovered from the SIX1/2 motif. A comparative analysis of tumor and developmental programs might identify regulatory networks and gene targets responsible for the persistence of these tumor cells through chemotherapy treatment.

## MATERIALS AND METHODS

### Mouse and human kidney samples

All surgical procedures, mouse handling and husbandry were performed according to guidelines issued by the Institutional Animal Care and Use Committees (IACUC) at the University of Southern California and after approval from the institutional IACUC committee. Mouse strains utilized are described in supplementary Materials and Methods. De-identified human fetal kidney tissues ranging from 16-17 weeks gestation were obtained from Novogenix Laboratories following informed consent and elective termination. Developmental age was determined by ultrasound.

### ChIP-seq

ChIP-seq from E16.5 mouse kidney tissue was performed essentially as described (Park et al., 2012). For ChIP-seq from human fetal kidneys, samples were microdissected to remove the cortex and incubated for 30 min at room temperature in crosslink buffer (Park et al., 2012). Crosslinking was stopped by the addition of glycine. Tissue was washed with PBS containing protease inhibitors (PI), homogenized, pelleted, and lysed in mouse ChIP lysis buffer with the aid of a B Dounce homogenizer. Processing of the samples from this point was carried out using the mouse ChIP protocol. ChIP was performed with antibodies listed in Table S1. Sequencing libraries for both mouse and human ChIP DNA were made using the ThruPLEX-FD Prep Kit (Rubicon Genomics). Libraries were sequenced at the USC Epigenome Center on the Illumina HiSeq 2000.

### Fluorescence activated cell sorting (FACS)

E15.5 kidneys from Cited1-nuc-TagRFP-T$^{+}$ embryos were isolated and processed for FACS as described (Park et al., 2012). To isolate ITGA8$^{+}$ cells from human fetal kidneys, the outer capsule was removed and kidneys incubated with Liberase (Roche) to remove the outer cortical cell layers. Cell suspensions were incubated with anti-ITGA8 (R&D, AF4076) and appropriate Alexa Fluor-labeled secondary antibody. Sorting was performed on a BD FACSAria II Flow Cytometer.

### RNA-seq

RNA was isolated from Cited1$^{+}$ and ITGA8$^{+}$ cells using the Qiagen RNeasy Micro Kit. RNA was submitted to the USC Epigenome Center for library preparation and sequencing on the Illumina HiSeq 2000. All RNA-Seq reads were aligned to hg19 or mm9 using the DNA Nexus and quantified to generate RPKM. RNA-seq data are available on the Gene Expression Omnibus (accession number GSE73867) and summary data are listed in Table S1.

### Transgenic analysis of enhancer regions

G0 transgenic analysis was performed as previously described (Park et al., 2012). Details of enhancer construction and coordinates are described in the supplementary Materials and Methods. Samples were stained with X-gal, fixed and photographed using a Nikon SMZ 1500 fluorescent microscope. For sections, stained kidneys were cryosectioned and immunostained as described below.

### Immunofluorescence

16 week human fetal kidneys were fixed overnight. Mouse whole embryos or urogenital systems were fixed for 1 h. Human or mouse cryosections were immunostained as previously described (Mugford et al., 2008). Antibodies and dilutions are detailed in the supplementary Materials and Methods. Whole kidney images were captured on the Zeiss Axio Scan.Z1 Slide Scanner. All other images were acquired on a Nikon Eclipse 90i epi-fluorescent microscope, Zeiss LSM 780 inverted confocal microscope, or Leica TCS SP8 confocal. Slides from transfections were fixed and stained similarly using SIX1-specific, SIX2-specific or SIX2 crossreactive antibodies.

### Immunoprecipitation analysis

HEK293 cells were transfected with pTARGET-SIX2-3×FLAG-P2A-mCherry, pCIG-SIX1-Myc, pCIG-EYA1-Myc, or the appropriate control empty vector. Details of construct generation and transfection can be found in the supplementary Materials and Methods. Nuclear lysates were prepared using the Active Motif Nuclear Complex Co-IP Kit. Extracts were incubated overnight at 4°C with anti-FLAG (F3165, SIGMA) antibody bound to Dynabeads Protein G (Life Technologies). Beads were washed six times following the Co-IP kit protocol with recommended high-stringency conditions. Samples were resolved on a 10% SDS-PAGE gel, transferred to nitrocellulose and subjected to standard western blotting protocols using anti-FLAG or anti-Myc antibodies. For tissue co-immunoprecipitations, the outer cortex of 17 week human fetal kidneys was microdissected and a nuclear lysate prepared. Normal rabbit IgG, SIX1 (Cell Signaling) or SIX2 (MyBioSource) antibodies were crosslinked with dimethyl pimelimidate to Dynabeads Protein G using the Protein A/G SpinTrap Buffer Kit (GE Healthcare). Nuclear extracts were incubated overnight with antibody cross-linked beads at 4°C. Samples were washed five times with TBS+0.1% Triton X-100 and proteins eluted with 0.1 M Glycine-HCl, pH 2.9. Samples were treated as above for western blots. Antibodies against SIX1 (1:1000) and SIX2 (1:1000) were used for detection.

### ChIP-seq data analysis

All ChIP-seq sequences were mapped to hg19 or mm9 using Novoalign software (Novocraft). Mapped ChIP-seq and input data were analyzed using QuEST 2.4 software (Valouev et al., 2008). Mouse binding sites were converted to human sites using the liftOver utility (Rhead et al., 2010) available at the UCSC genome browser website. ChIP summary data is listed in Table S1. Human SIX1/SIX2 and mouse Six2 motifs were calculated using MEME *de novo* motif finder (Bailey et al., 2009). To assess the evolutionary conservation of the motif sites, we retrieved the cross-species 'PhyloP' conservation scores from the UCSC genome browser (Siepel et al., 2006). GREAT GO analysis was performed using the online GREAT program v2.0 (McLean et al., 2010). DAVID (Huang et al., 2007) was used on target genes from the analysis human and mouse binding site overlap. Assignment of target genes was performed by associating peaks with genes using GREAT (McLean et al., 2010). More specific details of parameters used are described in the supplementary Materials and Methods. ChIP-Seq data are available on the Gene Expression Omnibus under GSE73867.

#### Acknowledgements

The authors thank Dr Joo-Seop Park for helping develop the mouse whole kidney ChIP protocol and members of the McMahon Lab for critical discussion of the data. We thank Zayed Albertyn and Colin Hercus for their help with Novoalign.

#### Competing interests

The authors declare no competing or financial interests.

#### Author contributions

L.L.O. and A.P.M. designed the experiments. L.L.O. performed all experiments except the nephron progenitor RNA-seq (J.-D.B.), pronuclear injections (Y.L.), and

Development (2016) 143, 595-608 doi:10.1242/dev.127175

HEK293 construct generation and transfection (Q.G.). T.T. helped with the human immunostaining and P.H.W. helped with the ITGA8 FACS. Q.G. and A.V. designed and performed bioinformatics analyses. L.L.O., Q.G., A.V. and A.P.M. analyzed the data. L.L.O., Q.G., A.V. and A.P.M. prepared the manuscript.

**Funding**

Work in A.P.M.'s laboratory was supported by grants from the National Institutes of Health [DK054364 and DK094526]. Q.G. was supported by a graduate student fellowship from the California Institute for Regenerative Medicine. Deposited in PMC for release after 12 months.

**Supplementary information**

Supplementary information available online at
http://dev.biologists.org/lookup/suppl/doi:10.1242/dev.127175/-/DC1

**References**

**Abdelhak, S., Kalatzis, V., Heilig, R., Compain, S., Samson, D., Vincent, C., Weil, D., Cruaud, C., Sahly, I., Leibovici, M. et al.** (1997). A human homologue of the Drosophila eyes absent gene underlies branchio-oto-renal (BOR) syndrome and identifies a novel gene family. *Nat. Genet.* **15**, 157-164.

**Bailey, T. L., Bodén, M., Buske, F. A., Frith, M., Grant, C. E., Clementi, L., Ren, J., Li, W. W., and Noble, W. S.** (2009) MEME SUITE: tools for motif discovery and searching. *Nucleic Acids Res.* **37**, W202-W208.

**Barak, H., Huh, S. H., Chen, S., Jeanpierre, C., Martinovic, J., Parisot, M., Bole-Feysot, C., Nitschké, P., Salomon, R., Antignac, C. et al.** (2012). FGF9 and FGF20 maintain the stemness of nephron progenitors in mice and man. *Dev. Cell* **22**, 1191-1207.

**Bertram, J., Douglas-Denton, R. N., Diouf, B., Hughson, M. and Hoy, W.** (2011). Human nephron number: implications for health and disease. *Pediatr. Nephrol.* **26**, 1529-1533.

**Boyle, S., Shioda, T., Perantoni, A. O., and de Caestecker, M.** (2007). Cited1 and Cited2 are differentially expressed in the developing kidney but are not required for nephrogenesis. *Dev. Dyn.* **236**, 2321-2330.

**Boyle, S., Misfeldt, A., Chandler, K. J., Deal, K. K., Southard-Smith, E. M., Mortlock, D. P., Baldwin, H. S. and de Caestecker, M.** (2008). Fate mapping using Cited1-CreERT2 mice demonstrates that the cap mesenchyme contains self-renewing progenitor cells and gives rise exclusively to nephronic epithelia. *Dev. Biol.* **313**, 234-245.

**Brenner, B. M., Garcia, D. L. and Anderson, S.** (1988). Glomeruli and blood pressure: less of one, more the other? *Am. J. Hypertens.* **1**, 335-347.

**Brodbeck, S., Besenbeck, B. and Englert, C.** (2004). The transcription factor Six2 activates expression of the Gdnf gene as well as its own promoter. *Mech. Dev.* **121**, 1211-1222.

**Buller, C., Xu, X., Marquis, V., Schwanke, R. and Xu, P.-X.** (2001). Molecular effects of Eya1 domain mutations causing organ defects in BOR syndrome. *Hum. Mol. Genet.* **10**, 2775-2781.

**Cain, J. E., Hartwig, S., Bertram, J. F., and Rosenblum, N. D.** (2008). Bone morphogenetic protein signaling in the developing kidney: present and future. *Differentiation* **76**, 831-842.

**Carroll, T. J., Park, J.-S., Hayashi, S., Majumdar, A. and McMahon, A. P.** (2005). Wnt9b plays a central role in the regulation of mesenchymal to epithelial transitions underlying organogenesis of the mammalian urogenital system. *Dev. Cell* **9**, 283-292.

**Cheng, Y., Ma, Z., Kim, B.-H., Wu, W., Cayting, P., Boyle, A. P., Sundaram, V., Xing, X., Dogan, N., Li, J. et al.** (2014). Principles of regulatory information conservation between mouse and human. *Nature* **515**, 371-375.

**Cheyette, B. N. R., Green, P. J., Martin, K., Garren, H., Hartenstein, V. and Zipursky, S. L.** (1994). The Drosophila sine oculis locus encodes a homeodomain-containing protein required for the development of the entire visual system. *Neuron* **12**, 977-996.

**Clark, I. B. N., Boyd, J., Hamilton, G., Finnegan, D. J. and Jarman, A. P.** (2006). D-six4 plays a key role in patterning cell identities deriving from the Drosophila mesoderm. *Dev. Biol.* **294**, 220-231.

**Cullen-McEwen, L. A., Kett, M. M., Dowling, J., Anderson, W. P. and Bertram, J. F.** (2003). Nephron number, renal function, and arterial pressure in aged GDNF heterozygous mice. *Hypertension* **41**, 335-340.

**Davidson, A. J.** (2009). Mouse kidney development. The Stem Cell Research Community, StemBook. doi/10.3824/stembook.1.34.1.

**Fischbach, K. F. and Heisenberg, M.** (1981). Structural brain mutant of *Drosophila melanogaster* with reduced cell number in the medulla cortex and with normal optomotor yaw response. *Proc. Natl. Acad. Sci. USA* **78**, 1105-1109.

**Fischbach, K. F. and Technau, G.** (1984). Cell degeneration in the developing optic lobes of the sine oculis and small-optic-lobes mutants of *Drosophila melanogaster*. *Dev. Biol.* **104**, 219-239.

**Gong, K.-Q., Yallowitz, A. R., Sun, H., Dressler, G. R. and Wellik, D. M.** (2007). A Hox-Eya-Pax complex regulates early kidney developmental gene expression. *Mol. Cell. Biol.* **27**, 7661-7668.

**Hartman, H. A., Lai, H. L. and Patterson, L. T.** (2007). Cessation of renal morphogenesis in mice. *Dev. Biol.* **310**, 379-387.

**Hendry, C. E., Vanslambrouck, J. M., Ineson, J., Suhaimi, N., Takasato, M., Rae, F. and Little, M. H.** (2013). Direct transcriptional reprogramming of adult cells to embryonic nephron progenitors. *J. Am. Soc. Nephrol.* **24**, 1424-1434.

**Hinchliffe, S. A., Sargent, P. H., Howard, C. V., Chan, Y. F. and van Velzen, D.** (1991). Human intrauterine renal growth expressed in absolute number of glomeruli assessed by the disector method and Cavalieri principle. *Lab. Invest.* **64**, 777-784.

**Huang, D. W., Sherman, B. T., Tan, Q., Kir, J., Liu, D., Bryant, D., Guo, Y., Stephens, R., Baseler, M. W., Lane, H. C. and Lempicki, R. A.** (2007). DAVID Bioinformatics Resources: expanded annotation database and novel algorithms to better extract biology from large gene lists. *Nucleic Acids Res.* **35**, W169-W175.

**Hughson, M., Farris, A. B., III, Douglas-Denton, R., Hoy, W. E. and Bertram, J. F.** (2003). Glomerular number and size in autopsy kidneys: the relationship to birth weight. *Kidney Int.* **63**, 2113-2122.

**Hughson, M. D., Douglas-Denton, R., Bertram, J. F. and Hoy, W. E.** (2006). Hypertension, glomerular number, and birth weight in African Americans and white subjects in the southeastern United States. *Kidney Int.* **69**, 671-678.

**Humbert, C., Silbermann, F., Morar, B., Parisot, M., Zarhrate, M., Masson, C., Tores, F., Blanchet, P., Perez, M.-J., Petrov, Y. et al.** (2014). Integrin alpha 8 recessive mutations are responsible for bilateral renal agenesis in humans. *Am. J. Hum. Genet.* **94**, 288-294.

**James, R. G., Kamei, C. N., Wang, Q., Jiang, R. and Schultheiss, T. M.** (2006). Odd-skipped related 1 is required for development of the metanephric kidney and regulates formation and differentiation of kidney precursor cells. *Development* **133**, 2995-3004.

**Kanda, S., Tanigawa, S., Ohmori, T., Taguchi, A., Kudo, K., Suzuki, Y., Sato, Y., Hino, S., Sander, M., Perantoni, A. O. et al.** (2014). Sall1 maintains nephron progenitors and nascent nephrons by acting as both an activator and a repressor. *J. Am. Soc. Nephrol.* **25**, 2584-2595.

**Karner, C. M., Das, A., Ma, Z., Self, M., Chen, C., Lum, L., Oliver, G. and Carroll, T. J.** (2011). Canonical Wnt9b signaling balances progenitor cell expansion and differentiation during kidney development. *Development* **138**, 1247-1257.

**Keller, G., Zimmer, G., Mall, G., Ritz, E. and Amann, K.** (2003). Nephron number in patients with primary hypertension. *N. Engl. J. Med.* **348**, 101-108.

**Kenyon, K. L., Yang-Zhou, D., Cai, C. Q., Tran, S., Clouser, C., Decene, G., Ranade, S. and Pignoni, F.** (2005). Partner specificity is essential for proper function of the six-type homeodomain proteins sine oculis and optix during fly eye development. *Dev. Biol.* **286**, 158-168.

**Kirby, R. J., Hamilton, G. M., Finnegan, D. J., Johnson, K. J. and Jarman, A. P.** (2001). Drosophila homolog of the myotonic dystrophy-associated gene, six5, is required for muscle and gonad development. *Curr. Biol.* **11**, 1044-1049.

**Kobayashi, A., Valerius, M. T., Mugford, J. W., Carroll, T. J., Self, M., Oliver, G. and McMahon, A. P.** (2008). Six2 defines and regulates a multipotent self-renewing nephron progenitor population throughout mammalian kidney development. *Cell Stem Cell* **3**, 169-181.

**Kohlhase, J., Wischermann, A., Reichenbach, H., Froster, U., and Engel, W.** (1998). Mutations in the SALL1 putative transcription factor gene cause Townes-Brocks syndrome. *Nat. Genet.* **18**, 81-83.

**Kreidberg, J. A., Sariola, H., Loring, J. M., Maeda, M., Pelletier, J., Housman, D. and Jaenisch, R.** (1993). WT-1 is required for early kidney development. *Cell* **74**, 679-691.

**Kumar, J. P.** (2009). The sine oculis homeobox (SIX) family of transcription factors as regulators of development and disease. *Cell. Mol. Life Sci.* **66**, 565-583.

**Kunarso, G., Chia, N.-Y., Jeyakani, J., Hwang, C., Lu, X., Chan, Y.-S., Ng, H.-H. and Bourque, G.** (2010). Transposable elements have rewired the core regulatory network of human embryonic stem cells. *Nat. Genet.* **42**, 631-634.

**Li, C.-M., Guo, M., Borczuk, A., Powell, C. A., Wei, M., Thaker, H. M., Friedman, R., Klein, U. and Tycko, B.** (2002). Gene expression in Wilms' tumor mimics the earliest committed stage in the metanephric mesenchymal-epithelial transition. *Am. J. Pathol.* **160**, 2181-2190.

**Li, X., Oghi, K. A., Zhang, J., Krones, A., Bush, K. T., Glass, C. K., Nigam, S. K., Aggarwal, A. K., Maas, R., Rose, D. W. et al.** (2003). Eya protein phosphatase activity regulates Six1–Dach–Eya transcriptional effects in mammalian organogenesis. *Nature* **426**, 247-254.

**Liu, Y., Nandi, S., Martel, A., Antoun, A., Ioshikhes, I. and Blais, A.** (2012). Discovery, optimization and validation of an optimal DNA-binding sequence for the Six1 homeodomain transcription factor. *Nucl. Acids Res.* **40**, 8227-8239.

**Lovvorn, H. N., Westrup, J., Opperman, S., Boyle, S., Shi, G., Anderson, J., Perlman, E. J., Perantoni, A. O., Wills M. and de Caestecker, M.** (2007). CITED1 expression in Wilms' tumor and embryonic kidney. *Neoplasia* **9**, 589-600.

**Mañalich, R., Reyes, L., Herrera, M., Melendi, C. and Fundora, I.** (2000). Relationship between weight at birth and the number and size of renal glomeruli in humans: a histomorphometric study. *Kidney Int.* **58**, 770-773.

**McLean, C. Y., Bristor, D., Hiller, M., Clarke, S. L., Schaar, B. T., Lowe, C. B., Wenger, A. M. and Bejerano, G.** (2010). GREAT improves functional interpretation of cis-regulatory regions. *Nat. Biotechnol.* **28**, 495-501.

**Milani, R.** (1941). Two new eye-shape mutant alleles in *Drosophila melanogaster*. *DIS* **14**, 52.

**Motamedi, F. J., Badro, D. A., Clarkson, M., Rita Lecca, M., Bradford, S. T., Buske, F. A., Saar, K., Hübner, N., Brändli, A. W. and Schedl, A.** (2014). WT1 controls antagonistic FGF and BMP-pSMAD pathways in early renal progenitors. *Nat. Commun.* **5**, 4444.

**Mugford, J. W., Sipilä, P., Kobayashi, A., Behringer, R. R. and McMahon, A. P.** (2008). Hoxd11 specifies a program of metanephric kidney development within the intermediate mesoderm of the mouse embryo. *Dev. Biol.* **319**, 396-405.

**Mugford, J. W., Yu, J., Kobayashi, A. and McMahon, A. P.** (2009). High-resolution gene expression analysis of the developing mouse kidney defines novel cellular compartments within the nephron progenitor population. *Dev. Biol.* **333**, 312-323.

**Müller, U., Wang, D., Denda, S., Meneses, J. J., Pedersen, R. A. and Reichardt, L. F.** (1997). Integrin alpha8beta1 is critically important for epithelial–mesenchymal interactions during kidney morphogenesis. *Cell* **88**, 603-613.

**Murphy, A. J., Pierce, J., de Caestecker, C., Taylor, C., Anderson, J. R., Perantoni, A. O., de Caestecker, M. P. and Lovvorn, H. N.III** (2012). SIX2 and CITED1, markers of nephronic progenitor self-renewal, remain active in primitive elements of Wilms' tumor. *J. Pediatr. Surg.* **47**, 1239-1249.

**Nishinakamura, R., Matsumoto, Y., Nakao, K., Nakamura, K., Sato, A., Copeland, N. G., Gilbert, D. J., Jenkins, N. A., Scully, S., Lacey, D. L. et al.** (2001). Murine homolog of SALL1 is essential for ureteric bud invasion in kidney development. *Development* **128**, 3105-3115.

**Odom, D. T., Dowell, R. D., Jacobsen, E. S., Gordon, W., Danford, T. W., MacIsaac, K. D., Rolfe, P. A., Conboy, C. M., Gifford, D. K. and Fraenkel, E.** (2007). Tissue-specific transcriptional regulation has diverged significantly between human and mouse. *Nat. Genet.* **39**, 730-732.

**Oliver, G., Wehr, R., Jenkins, N. A., Copeland, N. G., Cheyette, B. N., Hartenstein, V., Zipursky, S. L. and Gruss, P.** (1995). Homeobox genes and connective tissue patterning. *Development* **121**, 693-705.

**Park, J.-S., Ma, W., O'Brien, L. L., Chung, E., Guo, J.-J., Cheng, J.-G., Valerius, M. T., McMahon, J. A., Wong, W. H. and McMahon, A. P.** (2012). Six2 and Wnt regulate self-renewal and commitment of nephron progenitors through shared gene regulatory networks. *Dev. Cell* **23**, 637-651.

**Pignoni, F., Hu, B., Zavitz, K. H., Xiao, J., Garrity, P. A. and Zipursky, S. L.** (1997). The eye-specification proteins so and eya form a complex and regulate multiple steps in Drosophila eye development. *Cell* **91**, 881-891.

**Rhead, B., Karolchik, D., Kuhn, R. M., Hinrichs, A. S., Zweig, A. S., Fujita, P. A., Diekhans, M., Smith, K. E., Rosenbloom, K. R., Raney, B. J. et al.** (2010). The UCSC Genome Browser database: update 2010. *Nucleic Acids Res.* **38**, D613-D619.

**Rodríguez-Soriano, J., Aguirre, M., Oliveros, R. and Vallo, A.** (2005). Long-term renal follow-up of extremely low birth weight infants. *Pediatr. Nephrol.* **20**, 579-584.

**Ruf, R. G., Xu, P.-X., Silvius, D., Otto, E. A., Beekmann, F., Muerb, U. T., Kumar, S., Neuhaus, T. J., Kemper, M. J., Raymond, R. M., Jr** et al. (2004). SIX1 mutations cause branchio-oto-renal syndrome by disruption of EYA1-SIX1-DNA complexes. *Proc. Natl. Acad. Sci. USA* **101**, 8090-8095.

**Rumballe, B. A., Georgas, K. M., Combes, A. N., Ju, A. L., Gilbert, T. and Little, M. H.** (2011). Nephron formation adopts a novel spatial topology at cessation of nephrogenesis. *Dev. Biol.* **360**, 110-122.

**Sato, S., Ikeda, K., Shioi, G., Nakao, K., Yajima, H. and Kawakami, K.** (2012). Regulation of Six1 expression by evolutionarily conserved enhancers in tetrapods. *Dev. Biol.* **368**, 95-108.

**Schmidt, D., Wilson, M. D., Ballester, B., Schwalie, P. C., Brown, G. D., Marshall, A., Kutter, C., Watt, S., Martinez-Jimenez, C. P., Mackay, S. et al.** (2010). Five-vertebrate ChIP-seq reveals the evolutionary dynamics of transcription factor binding. *Science* **328**, 1036-1040.

**Sehic, D., Karlsson, J., Sandstedt, B. and Gisselsson, D.** (2012). SIX1 protein expression selectively identifies blastemal elements in Wilms tumor. *Pediatr. Blood Cancer* **59**, 62-68.

**Sehic, D., Ciornei, C. D. and Gisselsson, D.** (2014). Evaluation of CITED1, SIX1, and CD56 protein expression for identification of blastemal elements in Wilms tumor. *Am. J. Clin. Pathol.* **141**, 828-833.

**Seimiya, M. and Gehring, W. J.** (2000). The Drosophila homeobox gene optix is capable of inducing ectopic eyes by an eyeless-independent mechanism. *Development* **127**, 1879-1886.

**Self, M., Lagutin, O. V., Bowling, B., Hendrix, J., Cai, Y., Dressler, G. R. and Oliver, G.** (2006). Six2 is required for suppression of nephrogenesis and progenitor renewal in the developing kidney. *EMBO J.* **25**, 5214-5228.

**Senanayake, U., Koller, K., Pichler, M., Leuschner, I., Strohmaier, H., Hadler, U., Das, S., Hoefler, G. and Guertl, B.** (2013). The pluripotent renal stem cell regulator SIX2 is activated in renal neoplasms and influences cellular proliferation and migration. *Hum. Pathol.* **44**, 336-345.

**Seo, H.-C., Curtiss, J., Mlodzik, M. and Fjose, A.** (1999). Six class homeobox genes in Drosophila belong to three distinct families and are involved in head development. *Mech. Dev.* **83**, 127-139.

**Serikaku, M. A. and O'Tousa, J. E.** (1994). Sine oculis is a homeobox gene required for Drosophila visual system development. *Genetics* **138**, 1137-1150.

**Short, K. M., Combes, A. N., Lefevre, J., Ju, A. L., Georgas, K. M., Lamberton, T., Cairncross, O., Rumballe, B. A., McMahon, A. P., Hamilton, NA et al.** (2014). Global quantification of tissue dynamics in the developing mouse kidney. *Dev. Cell* **29**, 188-202.

**Siepel, A., Pollard, K. S. and Haussler, D.** (2006). New methods for detecting lineage-specific selection. *Res. Comput. Mol. Biol.* 3909, 190-205. Springer Berlin Heidelberg.

**Tang, Q., Chen, Y., Meyer, C., Geistlinger, T., Lupien, M., Wang, Q., Liu, T., Zhang, Y., Brown, M. and Liu, X. S.** (2011). A comprehensive view of nuclear receptor cancer cistromes. *Cancer Res.* **71**, 6940-6947.

**Torres, M., Gomez-Pardo, E., Dressler, G. R. and Gruss, P.** (1995). Pax-2 controls multiple steps of urogenital development. *Development* **121**, 4057-4065.

**Valouev, A., Johnson, D. S., Sundquist, A., Medina, C., Anton, E., Batzoglou, S., Myers, R. M. and Sidow, A.** (2008). Genome-wide analysis of transcription factor binding sites based on ChIP-Seq data. *Nat. Methods* **5**, 829-834.

**Walz, A. L., Ooms, A., Gadd, S., Gerhard, D. S., Smith, M. A., Guidry Auvil, J. M., Meerzaman, D., Chen, Q.-R., Hsu, C. H., Yan, C. et al.** (2015). Recurrent DGCR8, DROSHA, and SIX homeodomain mutations in favorable histology Wilms tumors. *Cancer Cell* **27**, 286-297.

**Weasner, B., Salzer, C. and Kumar, J. P.** (2007). Sine oculis, a member of the six family of transcription factors, directs eye formation. *Dev. Biol.* **303**, 756-771.

**Weber, S., Taylor, J. C., Winyard, P., Baker, K. F., Sullivan-Brown, J., Schild, R., Knuppel, T., Zurowska, A. M., Caldas-Alfonso, A., Litwin, M. et al.** (2008). SIX2 and BMP4 mutations associate with anomalous kidney development. *J. Am. Soc. Nephrol.* **19**, 891-903.

**Wegert, J., Ishaque, N., Vardapour, R., Geörg, C., Gu, Z., Bieg, M., Ziegler, B., Bausenwein, S., Nourkami, N., Ludwig, N. et al.** (2015). Mutations in the SIX1/2 pathway and the DROSHA/DGCR8 miRNA microprocessor complex underlie high-risk blastemal type Wilms tumors. *Cancer Cell* **27**, 298-311.

**Wellik, D. M., Hawkes, P. J. and Capecchi, M. R.** (2002). Hox11 paralogous genes are essential for metanephric kidney induction. *Genes Dev.* **16**, 1423-1432.

**Xu, J. and Xu, P. X.** (2015). Eya-Six are necessary for survival of nephrogenic cord progenitors and inducing nephric duct development prior to ureteric bud formation. *Dev. Dyn.* **7**, 866-873.

**Xu, P.-X., Adams, J., Peters, H., Brown, M. C., Heaney, S. and Maas, R.** (1999). Eya1-deficient mice lack ears and kidneys and show abnormal apoptosis of organ primordia. *Nat. Genet.* **23**, 113-117.

**Xu, P. X., Zheng, W., Laclef, C., Maire, P., Maas, R. L., Peters, H. and Xu, X.** (2002). Eya1 is required for the morphogenesis of mammalian thymus, parathyroid and thyroid. *Development* **129**, 3033-3044.

**Xu, P.-X., Zheng, W., Huang, L., Maire, P., Laclef, C. and Silvius, D.** (2003). Six1 is required for the early organogenesis of mammalian kidney. *Development* **130**, 3085-3094.

**Xu, J., Liu, H., Park, J.-S., Lan, Y. and Jiang, R.** (2014). Osr1 acts downstream of and interacts synergistically with Six2 to maintain nephron progenitor cells during kidney organogenesis. *Development* **141**, 1442-1452.

**Zou, D., Silvius, D., Fritzsch, B. and Xu, P.-X.** (2004). Eya1 and Six1 are essential for early steps of sensory neurogenesis in mammalian cranial placodes. *Development* **131**, 5561-5572.

## Supplemental Materials and Methods

*Mouse strains*

*Six2*$^{GCE/+}$ mouse lines were generated as previously described (Kobayashi et al., 2008) and maintained on a C57BL/6J (Jackson Laboratory) background. Wild type mice utilized for ChIP-seq and immunostaining were from Swiss Webster (Taconic) timed matings where noon on the day of vaginal plug detection is considered 0.5 days *post coitum*, or E0.5. *Cited1-nuc-TagRFP-T*$^{tg}$ animals (http://gudmap.org) were maintained as a homozygous breeding stock and mated to Swiss Webster females for timed collections. Transgenic analyses were performed using the hybrid B6SJLF1/J (Jackson Laboratory) strain.

*Transgenic analysis of enhancer regions*

A single copy of each enhancer was inserted via Gateway cloning methods into a modified Hsp68-lacZ::nGFP reporter construct (Tsanov et al. 2012). Enhancers were PCR amplified from genomic DNA or synthesized (Genewiz). Enh1 hg19 genomic coordinates: chr14:61,104,600-61,105,260. Enh2 hg19 genomic coordinates: chr14:61,119,745-61,119,994. Pronuclear injections were performed in house using standard protocols and injection of 2 ng/µl DNA into B6SJLF2 fertilized eggs.

*Antibodies and dilutions used for immunostaining*

SIX1 (1:500, Cell Signaling, 12891), SIX2 (1:1000, MyBioSource, MBS610128), CITED1 (1:250, Abnova, H00004435-M03 (Fig. S1A, Bottom); 1:500, Lab Vision, RB-9129 (Fig. S1A, Top)), JAG1 (1:250, R&D Systems, AF599), ECAD (1:250, BD Biosciences, 610181; 1:1000, Sigma, U3254), ITGA8 (1:500, R&D Systems, AF4076), GFP (1:500, AvesLabs, GFP-1020), cytokeratin (1:250, Sigma, C2931).

*Cell culture and transfections*

NIH3T3 or HEK293 cells (ATCC) were cultured in slide chambers or dishes, respectively, at 37$^{o}$C, 5% $CO_2$ in DMEM containing 10% FBS, 100 units/ml penicillin and 100 mg/ml streptomycin. SIX2 was amplified from 16 week fetal kidney cDNA and cloned into the pCS2+ plasmid using BamHI and EcoRI restriction sites (SIX2-pCS2). SIX2 was amplified with a 3XFLAG tag from this construct and inserted into pTARGET carrying a -P2A-mCherry cassette using BamHI and XhoI restriction sites. SIX1-pCMV6-XL5 was purchased from OriGene. SIX1 was amplified with a Myc tag and inserted into the pCIG vector using XhoI and ClaI sites. EYA1 was amplified from 16 week fetal kidney cDNA with a Myc tag and inserted into pCIG using EcoRI and XmaI sites. Empty vectors were used as controls. Transfections of all constructs were performed using Promega FuGENE HD transfection reagents following manufacturer protocols.

*ChIP-seq alignment and peak calling*

Novoalign (Novocraft) alignment parameters: Single-end reads trimming of 10 bp, polyclonal read filter: 7,10 0.4,2, maximum alignment score acceptable: 120. QuEST (Valouev et al., 2008) peak calling parameters: We used a "transcription factor" setting (for human SIX2, SIX1 and mouse Six2; bandwidth of 30 bp, regions size of 300 bp) or a 'histone' setting (for human H3K27ac, mouse H3K27me3 and H3K27ac; bandwidth of 100 bp, regions size of 1000 bp). Peak calling stringency was specified as following: a sample-dependent ChIP enrichment fold, 3-fold ChIP over input enrichment were used to seed the regions, and 3-fold ChIP enrichment was assigned for extending the regions. FDR for detecting the bound regions was evaluated by allocating the same number of mapped reads from a separate mouse input library and performing QuEST analysis using the same parameters.

*DNA sequence motif analysis*

MEME (Bailey et al., 2006) was run on a pool of 100 bp sequences obtained around the top 1000 most-enriched human SIX2, mouse Six2 or human SIX1 ChIP-seq peaks. Percentages of peaks with motif were calculated using FIMO tool (Grant et al., 2011) with p-value cutoff of 0.0002. We used binomial test to evaluate the statistical significance of motif enrichment within binding peaks.

*Calculation of regulatory scores*

In order to measure the potential of a gene being regulated by SIX2, we calculated regulatory score (*RS; adapted from Tang et al,. 2011*) for a given gene *g* ($RS_g$) using the following formula: $RS_g = \sum_p \frac{I_p}{(\max\{D_p,20000\})^{0.1}}$, where *p* is the ID of the peaks associated with gene g, and $D_p$ is the distance from peak *p* to the TSS of gene *g*. To select human/mouse-specific SIX2 target genes, regulatory scores were normalized to peak numbers and 75th quantile of peak intensity, then a z score was calculated based on Poisson distribution of regulatory score. Genes with z > 1 were selected as 'human/mouse-specific genes by SIX2 regulation'. These genes were further filtered for those with z > 5 fold expression in human vs. mouse (or vice versa) to generate the 'human/mouse-specific genes by both regulation and expression'.

*ChIP-Seq data comparison for mouse and human antibodies*

To compare the Six2 ChIP-Seq data generated using the Ab used in mouse Six2 ChIP-Seq (Six2_ms) and the in human SIX2 ChIP-Seq (Six2_hu), we generated 3 replicate ChIP-Seq data sets using each of the two Abs, respectively, in E16.5 mouse embryonic kidneys. After peak calling using QuEST, the peaks from all 3 replicates of each group were merged so that any peaks within 200 bp from each other are unioned, with the new coordinate being the midpoint of the original peak coordinates. Then ChIP-Seq

reads from each replicate were counted within +/-500 bp window around each peak. The read counts were transformed into enrichment fold (ChIP-Seq score, i.e. ((reads in 1 kb window)/1000 )/((total reads count)/(genome size))). We normalized the ChIP-Seq score for each replicate by bringing the median scores to the same number (practically, the maximum median). We performed pairwise comparison of the normalized data across replicates for Six2_ms and Six2_hu, respectively. To compare Six2_ms and Six2_hu data, we first merged the peaks from all six replicate data sets, and then calculated the ChIP-Seq score, which was subsequently normalized by bringing the medians of scores to the same number. Then we plotted the average ChIP-Seq score of Six2_ms vs. Six2_hu. Observing a subpopulation of peaks are skewed toward Six2_ms, we identified Six2_ms-specific sites by applying the threshold of Six2_ms score > 10 and Six2_cross score/Six2_spec score > 5. The reproducible peaks were defined as those with Six2_ms score > 10 and Six2_hu score > 10.

*Protein alignment*

Human and mouse SIX1/Six1 and SIX2/Six2 proteins were aligned using the ClustalW2 tool from the EMBL-EBI (Larkin et al., 2007). The SIX and Homeodomains were highlighted, and the amino acids that make DNA contacts marked (Kumar, 2009).

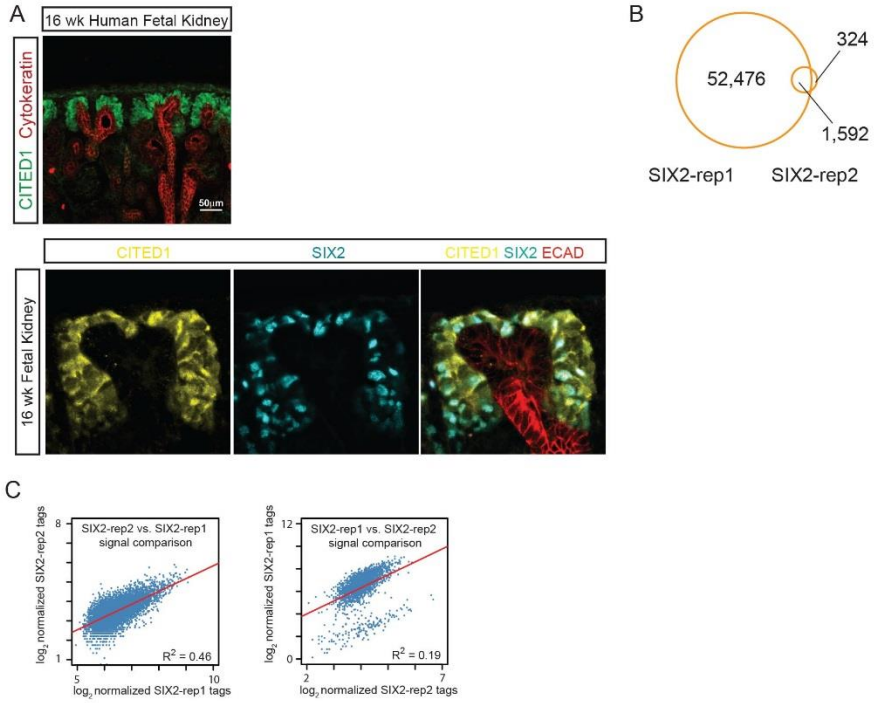


**Figure S1: CITED1 expression is similar to SIX2 and comparison of human SIX2 ChIP-seq replicates indicate rep1 is a stronger dataset.** (A) CITED1 and cytokeratin immunostaining of a 16 week human fetal kidney. Zoomed view of SIX2, CITED1, and ECAD co-staining shows overlap of SIX2 and CITED1 in nephron progenitors. (B) Venn diagram shows overlap between the two replicates of SIX2 ChIP-seq (SIX2-rep1, SIX2-rep2) peaks from independent 17 week human fetal kidneys. (C) Scatter plot shows correlation of SIX2-rep1 ChIP-seq reads and SIX2-rep2 within +/- 500 bp around SIX2-rep1 ChIP-seq peaks (left) and vice versa (right).

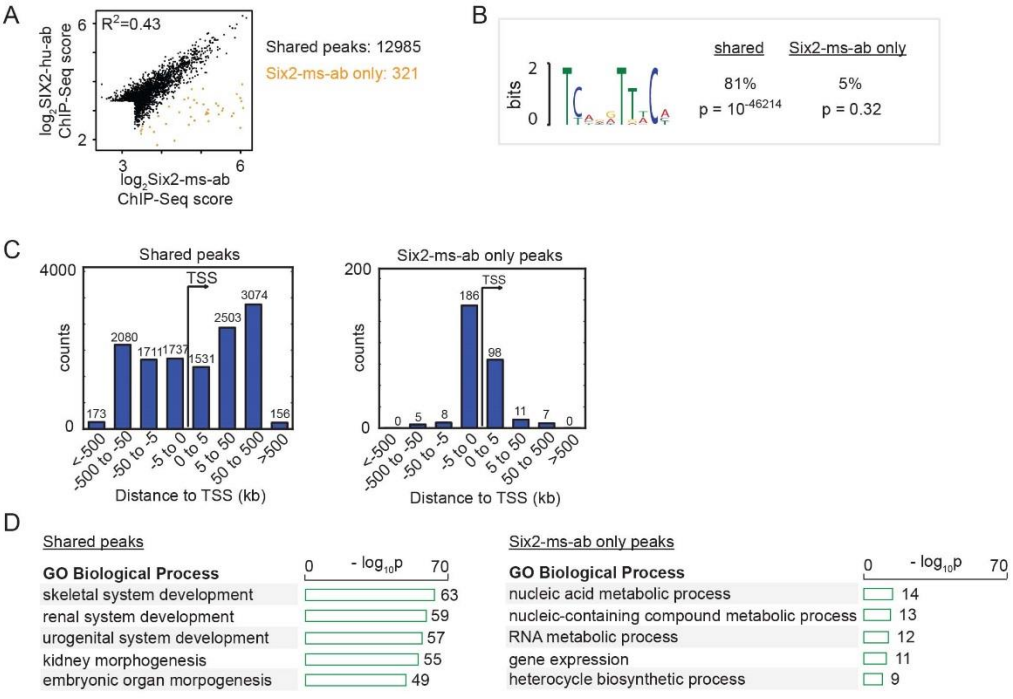


**Figure S2: Human and mouse SIX2/Six2 ChIP antibodies are comparable.** (A) Scatter plot shows comparison of Six2 ChIP-Seq data generated using the mouse Six2 ChIP antibody (Six2-ms-ab) or SIX2 human ChIP antibody (SIX2-hu-ab). Average enrichment fold (ChIP-Seq score) of replicate ChIP-Seq reads count within +/-500 bp of the indicated peaks were plotted. We identified 'shared peaks' and 'Six2-ms-ab only peaks' based on ChIP-Seq score, with metrics specified in the Methods. (B) Weblogo shows the most significantly enriched motif identified from +/-50 bp window of top 1000 shared peaks; no motif was identified from Six2-ms-ab only peaks. Percentages indicate frequency of the motif appearing in the indicated peaks. P-values indicate statistical significance of the frequency. (C) Histograms show distribution of distances of peaks to the nearest gene. (D) Barplots show enrichment of Gene Ontology (GO) terms for the shared peaks and Six2-ms-ab only peaks. The analysis was performed using the GREAT on-line tool (McLean et al., 2010).

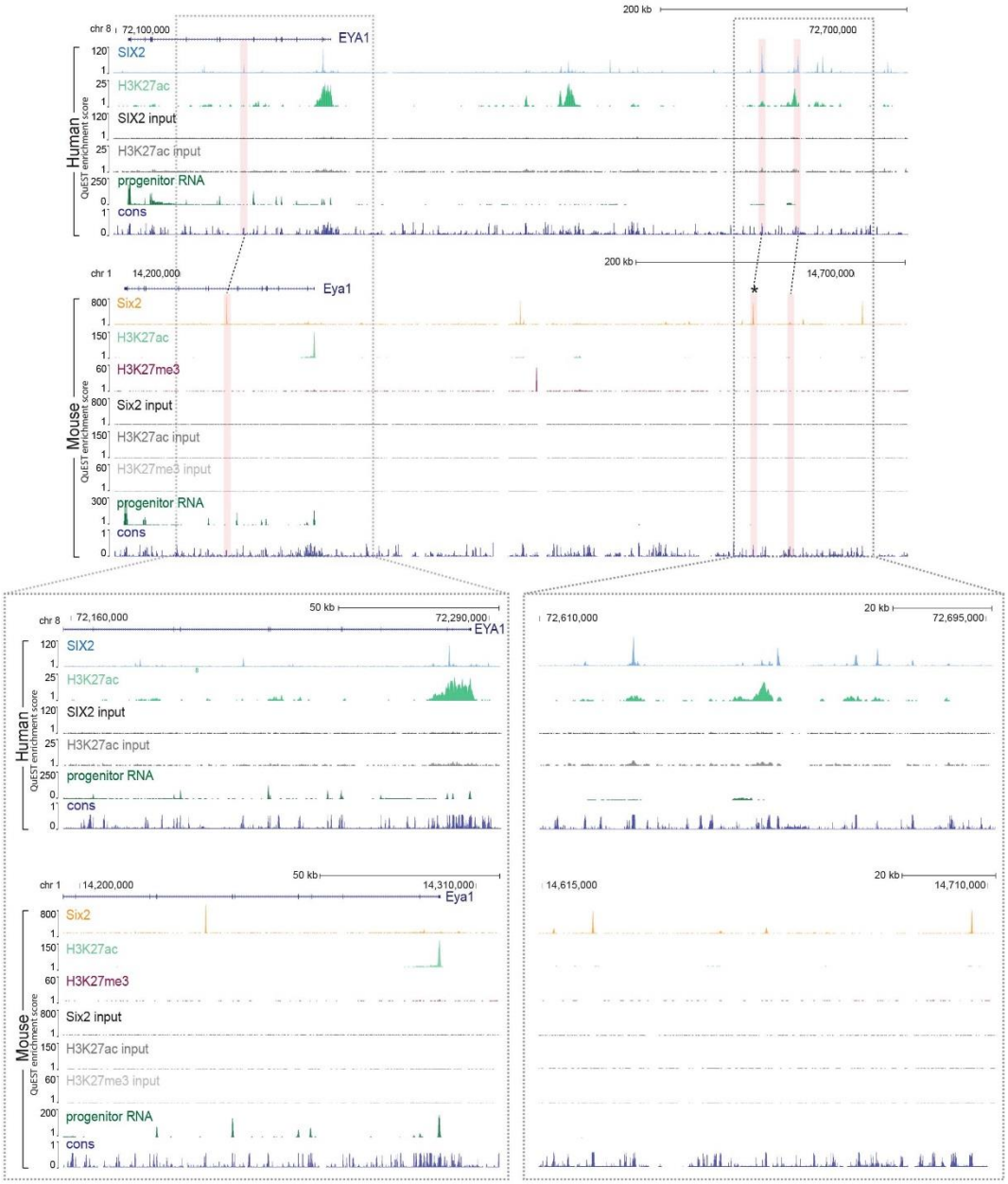


**Figure S3: Human and mouse SIX2 binding around EYA1 suggests EYA1 is key target of SIX regulation.** (A) Genomic view of human and mouse SIX2 binding near EYA1/Eya1 gene loci. Human tracks represent enrichment fold for SIX2 ChIP-seq, H3K27ac ChIP-seq and RNA-seq from ITGA8+ nephron progenitors, mouse tracks represent Six2 and H3K27ac ChIP-seq from E16.5 whole kidneys and H3K27me3 ChIP-seq and RNA-seq from Cited1+ nephron progenitors . 'Cons' track represents the Phastcon vertebrate conservation score. Highlighted regions are conserved from mouse to human. Mouse Six2 peak annotated with * was previously tested in a G0 transgenic assay and recapitulated Eya1 expression (Park et al., 2012).

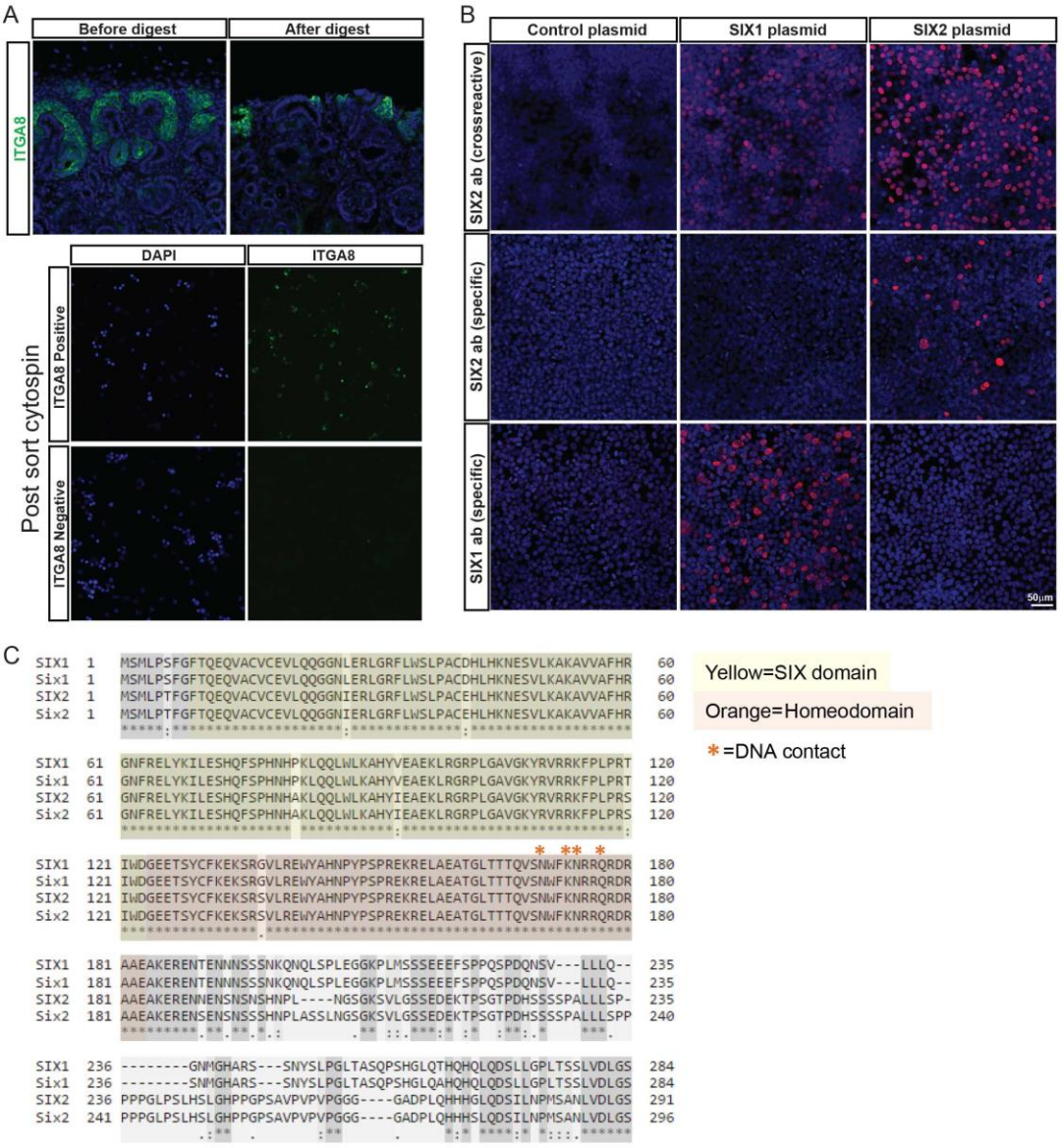


**Figure S4: ITGA8 in the human kidney, identification of SIX1 and SIX2 specific antibodies, and comparison of SIX1/Six1 and SIX2/Six2 protein.** (A) ITGA8 staining in a 16 week human fetal kidney before and after limited enzymatic digest for FACS showing the removal of the ITGA8+ nephron progenitors. Bottom panels show a cytospin sample cells collected from the ITGA8 positive FACS population or the negative population. (B) NIH3T3 cells were transfected with constructs to induce expression of SIX1 or SIX2. GFP was utilized as a control. Cells were stained with a SIX2 antibody raised against the full-length protein previously utilized for Six2 ChIP-seq (Park et al., 2012; top panel), a SIX2 antibody raised against a C-terminal epitope (aa264-277) (middle panel), and a SIX1 antibody raised against residues surrounding Pro249 (bottom panel). (C) Alignment of SIX1/Six1 and SIX2/Six2.

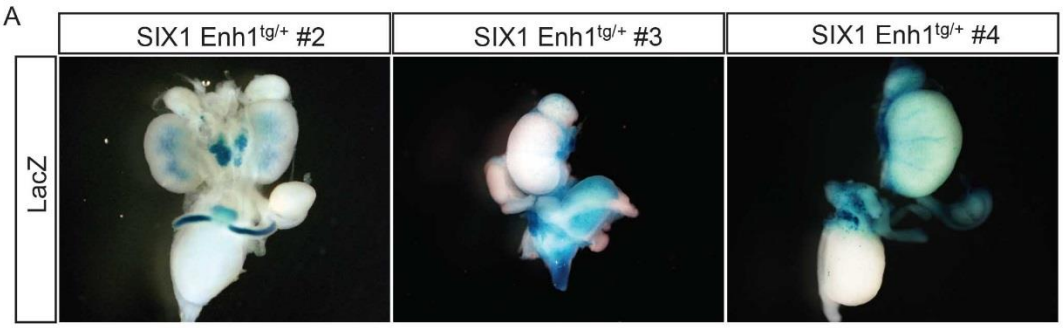


**Figure S5: Additional expression patterns observed from the injection of SIX1 Enhancer 1.** G0 transgenic analysis was performed at E15.5 and urogenital systems stained for LacZ reporter expression. Varied expression patterns are observed, with no two recapitulating the same pattern.

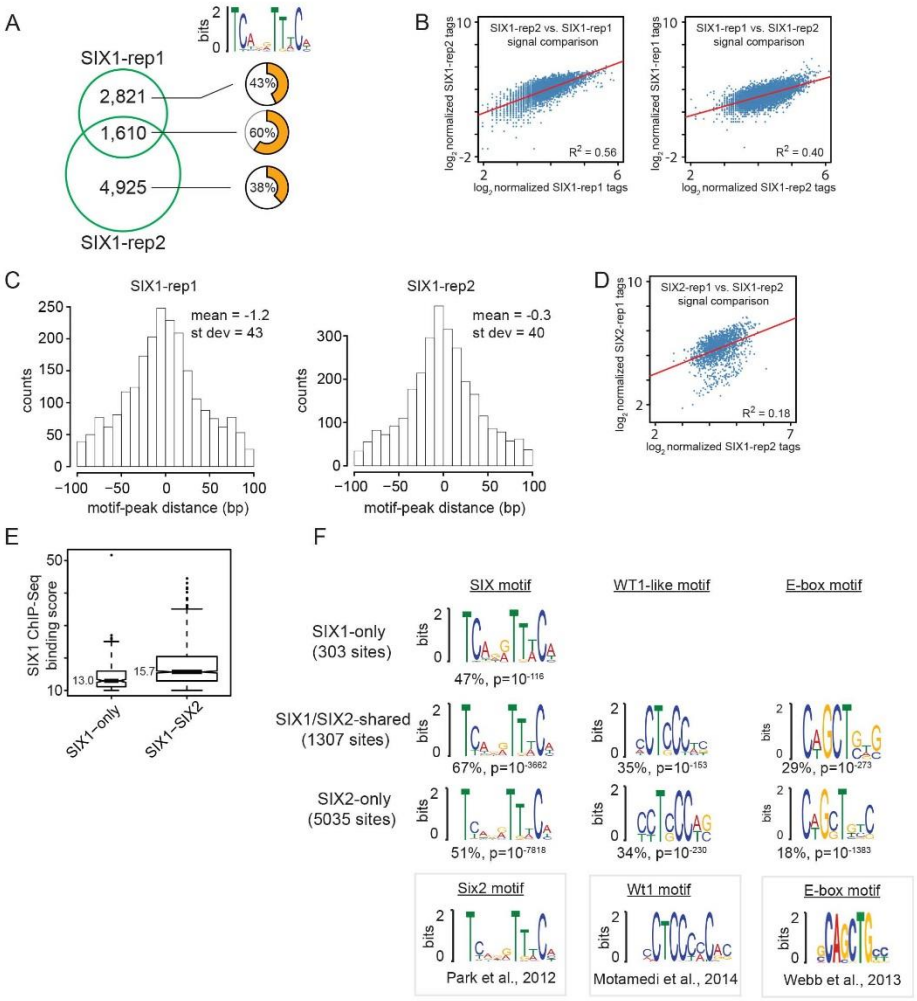


**Figure S6: Analysis of SIX1 ChIP-Seq replicates and SIX1/SIX2 ChIP-seq correlation.** (A) Venn diagram shows overlap (100 bp gap) between two replicates of SIX1 ChIP-seq peaks from 16 (rep1) and 17 week (rep2) human fetal kidneys. (B) Scatter plots show high correlation of the two SIX1 tag counts within SIX1-rep1 or SIX1-rep2 binding regions. (C) Histogram shows distribution of motif-peak distances of the SIX1 peaks from the two replicates. The motif is centered in both datasets, indicating direct association of SIX1 with the motif (D) Scatter plot shows a positive correlation of SIX1 and SIX2 reads within +/- 500 bp of SIX1 peaks. (E) Boxplot shows distribution of the ChIP-seq binding score for peaks unique to SIX1 (left) and SIX1 peaks overlapping with SIX2 and peaks (right). The size of the boxes are proportional to the square roots of the numbers of observations. Medians of each group are annotated on the left side of the boxes and indicate a higher binding score for those peaks that are shared between SIX1 and SIX2. (F) Motif discovery in SIX1-only, SIX2-only and SIX1/SIX2 co-binding sites.

**Table S1:** Details of samples, antibodies, and basic analyses for ChIP-seq and RNA-seq experiments.

| Sample name | Sample type | Species | Sample stage/tissue | ChIP Ab | Note | Mapped reads | Threshold | Peaks | FDR |
|---|---|---|---|---|---|---|---|---|---|
| SIX2-rep1 | ChIP-seq | Human | 17 week kidney cortex | SIX2 (MyBiosource; MBS610128) | Ab specific to SIX2 | 29120274 | 50 | 6275 | 0 |
| | | | | | | | 10 | 54068 | 0.02 |
| SIX2-rep2 | ChIP-seq | Human | 17 week kidney cortex | SIX2 (MyBiosource; MBS610128) | Ab specific to SIX2 | 25710785 | 10 | 1916 | 0.47 |
| SIX1-rep1 | ChIP-seq | Human | 16 week kidney cortex | SIX1 (Cell Signaling; 12891S) | Ab specific to SIX1 | 24821763 | 10 | 4431 | 0.11 |
| SIX1-rep2 | ChIP-seq | Human | 17 week kidney cortex | SIX1 (Cell Signaling; 12891S) | Ab specific to SIX1 | 26597952 | 10 | 6535 | 0.16 |
| H3K27ac | ChIP-seq | Human | 17 week kidney cortex | H3K27ac (Abcam, ab4729) | | 48190122 | NA | NA | NA |
| Six2 | ChIP-seq | Mouse | E16.5 whole kidney | SIX2 (Proteintech,11562-1-AP ) | Ab recognizes SIX1 and SIX2 | 30916440 | 60 | 12145 | 0.0003 |
| H3K27ac | ChIP-seq | Mouse | E16.5 whole kidney | H3K27ac (Abcam, ab4729) | | 213290495 | NA | NA | NA |
| H3K27me3 | ChIP-seq | Mouse | E16.5 Cited1+ cells | H3K27me3 (Abcam, ab6002) | | 213833317 | NA | NA | NA |
| Human-input1 | ChIP-seq | Human | 17 week kidney cortex | NA | | 44091209 | NA | NA | NA |
| Human-input2 | ChIP-seq | Human | 16 week kidney cortex | NA | | 40720333 | NA | NA | NA |
| Mouse-input | ChIP-seq | Mouse | E16.5 whole kidney | NA | | 19679957 | NA | NA | NA |
| Progenitor RNA | RNA-seq | Human | 17 week ITGA8+ | NA | | 11718597 | NA | NA | NA |
| Progenitor RNA | RNA-seq | Mouse | E15.5 Cited1+ cells | NA | | 57908653 | NA | NA | NA |

## Table S2

Click here to Download Table S2

## Table S3

Click here to Download Table S3

## Table S4

Click here to Download Table S4